Transmission of piezoelectrically induced sound in a liquid filled tube

Aleksi Öyry

School of Electrical Engineering

Thesis submitted for examination for the degree of Master of Science in Technology.

Espoo 9.2.2019

Thesis supervisor and advisor:

Prof. Ville Pulkki

Aalto University
School of Electrical
Engineering

AALTO UNIVERSITY
SCHOOL OF ELECTRICAL ENGINEERING

ABSTRACT OF THE
MASTER'S THESIS

Author: Aleksi Öyry

Title: Transmission of piezoelectrically induced sound in a liquid filled tube

Date: 9.2.2019 Language: English Number of pages: 7+47

Department of Signal Processing and Acoustics

Professorship: Acoustics and Audio Technology

Supervisor and advisor: Prof. Ville Pulkki

This thesis studies the transmission of piezoelectrically induced sound in a liquid-filled elastic tube. This type of sound transmission would be useful in functional Magnetic Resonance Imaging (fMRI), in which the strong magnetic fields prevent the use of typical electromagnetic sound sources. The liquid would act as hearing protection against powerful fMRI noise, while sound would be transmitted through the liquid to the test subject's eardrum.

In order to test this idea, a proof-of-concept measurement system was built including a waveguide, a tube and a sensor. The purpose of the experiment was to measure sound transmission through the tube. PVC tubes filled with viscous emulsion and water were measured. The results indicate that the pressure release-walled PVC tube and the liquid form a coupled system with complex vibrational behavior including longitudinal and transverse propagation modes. More research on the topic is required to determine whether or not the quality of sound transmission is sufficient for fMRI use.

Keywords: Acoustics, Sound Transmission, Liquid, Tube

AALTO-YLIOPISTO
SÄHKÖTEKNIIKAN KORKEAKOULU

DIPLOMITYÖN
TIIVISTELMÄ

Tekijä: Aleksi Öyry

Työn nimi: Piezosähköisesti tuotetun äänen eteneminen nesteellä täytetyssä putkessa

Päivämäärä: 9.2.2019 Kieli: Englanti Sivumäärä: 7+47

Signaalinkäsittelyn ja Akustiikan laitos

Professuuri: Akustiikka ja audiotekniikka

Työn valvoja: Prof. Ville Pulkki

Työn ohjaaja: Prof. Ville Pulkki

Tässä diplomityössä tutkitaan pietsosähköisesti tuotetun äänen etenemistä nesteellä täytetyssä elastisessa putkessa. Tämän kaltainen äänen välittyminen olisi hyödyllistä toiminnallisessa magneettikuvauksessa (fMRI), jossa voimakkaat magneettikentät estävät tyypillisten sähkömagneettisten äänilähteiden käytön. Neste voisi toimia kuulonsuojauksena fMRI-laitteen melua vastaan samalla, kun ääni kulkisi koehenkilön tärykalvolle nesteen kautta.

Idean kokeilemiseksi rakennettiin testilaitteisto aaltojohdosta, putkesta ja sensorista. Kokeen tarkoituksena oli mitata äänen etenemistä putkessa. Vedellä ja viskoosilla emulsiolla täytettyjä PVC-putkia mitattiin. Tulokset viittaavat siihen, että äänenpaineen vaikutuksesta muotoaan muuttava putki ja neste muodostavat monimutkaisen yhteen kytkeytyneen järjestelmän, jossa ääni etenee sekä pitkittäisenä, että poikittaisena aaltona. Lisätutkimusta tarvitaan, jotta saadaan selville äänenlaadun riittävyys fMRI-käytössä.

Avainsanat: Akustiikka, Äänen Eteneminen, Neste, Putki

Preface

When I begun my studies in electrical engineering in 2012 I was pretty sure that I would not graduate from Aalto University. In my thoughts I was going to pursue a career in music. Now seven years later I am very excited to become an acoustical engineer, though I still am pursuing that musical career at some level. There are many people who have helped me to finish this degree and I would like to give acknowledgement to all of them. Also the people who I am unable to mention below.

First of all, I want to thank prof. Ville Pulkki for giving me the opportunity to work on this interesting thesis topic and trusting me with the responsibilities of a lab engineer at the Acoustics Lab. His enthusiastic personality keeps the spirits high around the office. I also want to thank all my co-workers for their help. I want to thank my family for their sincere support in every aspect of my life. A special thank you goes to all of my friends and fellow students who kept me sane during my studies. I want to also thank the people involved in my music projects The Post, Stagement, PMPP and Valot for giving me the occasional and much needed distraction from writing this thesis.

Otaniemi, 9.2.2019

Aleksi J. Öyry

Contents

Symbols and abbreviations

AD	Analog to digital
DA	Digital to analog
dB	decibel
FFT	Fast Fourier transform
fMRI	functional Magnetic Resonance Imaging
PVC	Polyvinyl chloride
RMS	Root-mean-square
SNR	Signal-to-noise ratio
SPL	Sound pressure level

1 Introduction

The communication channel from a sound source to a listener is a complex phenomenon involving propagation of sound in a medium, effect of the human body and ear, hearing function in the inner ear and later processing in the brain. To better understand what happens in the nervous system when a sound is heard, the functioning of the brain should be measured. Neural activity in the brain caused by sound has been in the interest of researchers for decades.

The response of sound excitation can be measured in the brain activity for example in functional Magnetic Resonance Imaging (fMRI) by detecting changes in blood flow corresponding to the neural activity in the brain. In MRI scans, in which the function of the brain is not measured, a sound system can be used to communicate to the test subject during a scan sequence or music can be played to improve the comfort of the test subject.

The sound needs to be transmitted to the subjects ears in some manner. In normal conditions electromechanical transducers such as loudspeakers or headphones could be used, but in an MRI it is not possible because of the strong magnetic fields inside the machine. The magnetic fields of the transducers would also cause defects in the measurements. The ferromagnetic materials of the transducers could produce health hazards as the strong magnets of the scanner are able to make ferromagnetic objects move and even fly through the room at fast speeds. The existing MRI sound systems use piezoelectric transducers in a non-ferrous enclosure with plastic tubing connected to the enclosure and a headset inside the scanner [1].

MRI scanners produce a lot of noise. For example, an extreme case of a 4 Tesla MRI scanner is capable of producing a sound pressure level of up to 120-130 dB in the position of the head, while operating in echo-planar imaging (EPI) [2]. Typically the sound pressure levels are around 100 dB. For reference the sound pressure level of normal speech is in the range of 50-70 dB. The existing headsets are able to attenuate the noise by approximately 25 dB. Test subjects have found the test situation unpleasant because the noises include broadband, harmonic and non-harmonic, beating and knocking sound meanwhile they lay inside of a narrow tube. In addition, the ambient room noise is induced to the air-filled tube reducing the sound quality. The length of the tube must then be limited due to the induced airborne noise.

The scope of this work is to study the possibility of using a liquid-filled elastic tube for sound transmission with decent sound quality in an MRI scanner. Also the use of small scale piezo transducers as sound sources is a point of interest. The preliminary idea for the system is to fill also the test subjects ear canal with the same liquid up to the tympanic membrane. As the liquid should not drain out from inside the ear, strongly viscous liquids are of special interest in this study.

The primary effect for the liquid would be to act as hearing protection against the ambient room noise caused by the MRI scanner. The secondary effect is to function

as a medium for the sound to propagate in. The use of e.g. water based liquid would be beneficial as the ratio of acoustical impedance from air to water is about 3000, causing practically a perfect reflection [3]. In an experimental test in the MRI it was found that the subjects experienced the test situation much more comfortable when the ambient noise was blocked by gel in the ear canal. A boundary condition for the liquid used in the application is it's suitability to be inserted in human ear canals without generating any health hazards. Also the sound should be able to propagate several meters (up to 5-10 m) inside the tube.

The thesis is organized as follows: Section 2 covers fundamental acoustic phenomena and physics of sound as well as the function of hearing regarding the scope of this thesis. Section 3 covers the acoustical properties of liquids and solids in contrast to gaseous fluids. Additionally, different types of loss mechanisms in liquids are explained. Section 4 presents the piezoelectric effect and the piezoelectric electromechanical transducer types used in the practical part of this work. Section 5 describes the relevant acoustic phenomena related to sound propagation in liquid filled tubes. Differences between acoustically rigid walled and pressure release walled tubes are in the focal point. In section 6 the measurement methods and results are presented. Section 7 discusses the measurement results and gives outlook on the future work regarding the topic. Section 8 concludes the thesis.

2 Fundamental principles of sound and hearing

2.1 Physics of sound

As a physical phenomenon, sound manifests itself as time-dependent variations in the propagation medium. The variations are related to temperature, pressure, density and fluid particle positions and their moving velocities [4]. The total pressure p_{tot} of fluid particles is the static pressure p_{stat} and sound pressure p oscillates around this constant component described as

$$p_{\text{tot}} = p_{\text{stat}} + p. \tag{1}$$

As the dynamical range of sound is vast in Pascal units, it is more convenient to compare different *sound pressure levels* in decibels (dB), which is a logarithmic scale. The sound pressure level L_p is usually compared to a fixed reference and it is given by

$$L_p = 20 \ \log_{10}(\frac{p}{p_0}), \tag{2}$$

where p_0 is the reference pressure.

The vibrations of sound propagate as waves, usually in a fluid and they are often produced by a mechanical object. The speed of wave propagation, or sound velocity c is dependent of the temperature of the fluid. When the pressure changes and the particles oscillate, phase ϕ is what determines the observation point of the oscillation in the range [0 2π]. The number of these oscillations in a second is determined by frequency f in Hertz [Hz] and the distance of a full cycle in meters is a wave length λ [5]. The sound velocity can be calculated as

$$c = f\lambda. \tag{3}$$

2.2 Vibrating mass-spring systems

When a mechanical object is excited, the radiated sound may be boosted by *resonances* and attenuated by *losses* that transform the sound energy into another form [6]. The vibrating and sound radiating object can be described as a vibrating mass-spring system. The simplest harmonic system is a mass moving on a straight line which follows a sinusoidal function of time

$$x(t) = A\sin(2\pi f t), \tag{4}$$

where A is the amplitude, or maximum reach of motion and f the frequency of oscillation describing how often the motion is repeated. The period T, when the motion repeats in time as seconds is given by

$$T = \frac{1}{f}. \tag{5}$$

The simple sinusoidal oscillating system is presented in fig. 1.

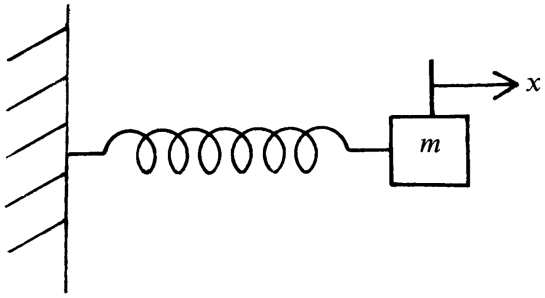

Figure 1: A simple sinusoidal oscillating mass-spring system. Adapted from [7].

When the system operates in harmonic limits, or in other words is not stretched too far, the amount of stretch x is proportional to the normalizing force. Assuming lossless conditions and combining Hooke's law $F = -kx$ and Newton's law of motion $F = ma = m\ddot{x}$, we get

$$m\ddot{x} = -kx \tag{6}$$

and

$$m\ddot{x} + kx = 0, \tag{7}$$

where $\ddot{x}$ is the second derivative of displacement x describing the acceleration of the mass and k is the stiffness or *spring constant*. Here m is the mass of the vibrating object. The natural angular frequency of the system is defined as $\omega_0 = \sqrt{k/m}$. Thus, the motion equation becomes

$$\ddot{x} + \omega_0^2 x = 0, \tag{8}$$

having the distinguished solutions

$$x = A\cos(\omega_0 t + \phi), \tag{9}$$

$$x = B\cos(\omega_0 t) + C\sin(\omega_0 t), \tag{10}$$

where ϕ is the initial phase and amplitude is $\sqrt{B^2 + C^2}$ or A. The eigen frequency of this simple oscillator is then $f_0 = (1/2\pi)\sqrt{k/m}$. [7]

In reality, all systems have losses such as viscous drag and sliding friction. The viscous drag force F_r for example is proportional to the velocity, leading to $F_r = -Rx$, where R is the mechanical resistance. The equation of motion then becomes

$$m\ddot{x} + R\dot{x} + kx = 0, \tag{11}$$

and the exponentially damped distinguished solutions will be

$$x = Ae^{-\alpha t}\cos(\omega_d t + \phi), \tag{12}$$

$$x = Be^{-\alpha t}\Big[\cos(\omega_d t) + C\sin(\omega_d t)\Big], \tag{13}$$

where $\alpha = R/m$ depicts the damping [6] [7]. The lossless and lossy oscillations with an initial displacement x_0 are presented in fig. 2.

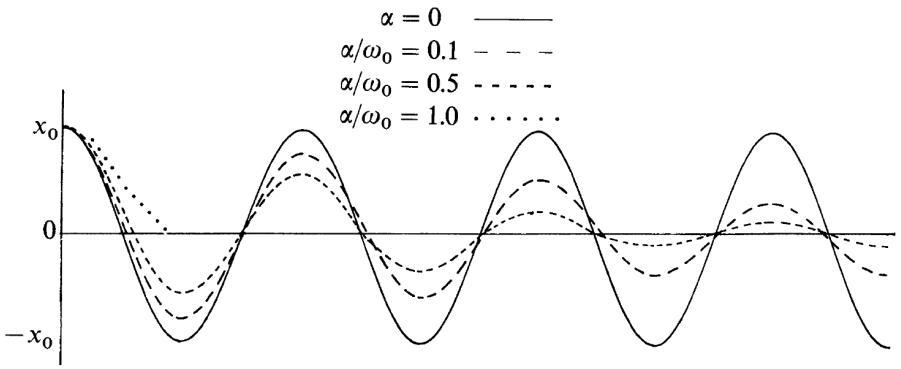

Figure 2: The lossless and lossy oscillation of a mass-spring system in time. Critical damping occurs when $\alpha \geq \omega_0$ Adapted from [7].

2.3 The human ear and hearing

A human being is capable of hearing sound with two ears. In hearing, the human ear captures the acoustical waves in the surrounding medium, transforms them into mechanical vibrations and further on converts the mechanical vibrations into neural signals. These neural impulses then travel to the brain where the sound is recognized.

2.3.1 Structure of the ear

The ear consists of three parts, the external, middle and inner ear. The structure of the ear is presented in fig. 3.

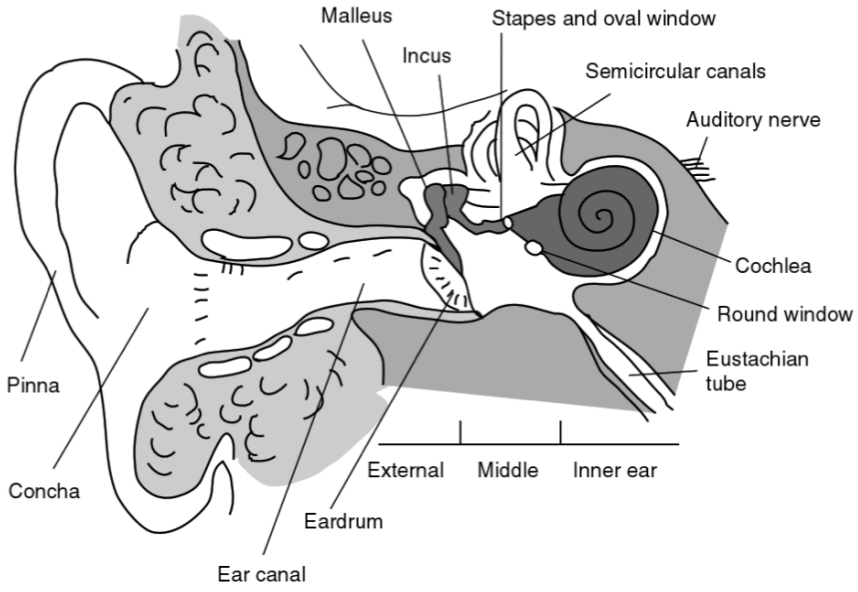

Figure 3: Structure of the ear. The ear can be divided into three parts, external, middle and inner ear. Adapted from [6].

The part that captures sound from surrounding medium is the external ear. External ear consists of the pinna, concha and ear canal, terminating to the tympanic membrane (eardrum) [8]. The pinna "disturbs" sound propagation at high frequencies giving monaural hints about the direction of the sound. Concha is the cavity that leads sound to the ear canal. Ear canal then directs the sound to the tympanic membrane. The canal has a diameter of approximately 7.5 mm and it is 22.5 cm long on average. It is essentially a quarter wave length resonator enhancing frequencies around 3-4 kHz. The tympanic membrane converts acoustic waves to mechanical vibrations for the middle ear [6].

After the sound is converted to mechanical vibrations by the tympanic membrane, the vibrations are forwarded to the inner ear by the *ossicles*, which are three little bones in an air cavity [8]. They act as a lever mechanism, that improves the impedance matching from air to water between external and inner ear. Small pressure and large velocity of the vibration is transformed to small velocity and large pressure. This is due to the area difference between the eardrum and oval window, which is the beginning of the inner ear. Middle ear also includes the *Eustachian tube*, which balances pressure between air and the middle ear [6].

The inner ear is comprised of the cochlea and semicircular canals. The cochlea is responsible for transforming mechanical vibrations from the middle ear to neural impulses. Semicircular canals, on the other hand, only act as a balance sensing organ. Structure of the cochlea is presented in fig. 4.

On the middle ear end of the cochlea, there are two ports, which are the round and oval window. The stapes is connected to a liquid inside of cochlea by the oval window. The whole cochlea is divided to two compartments by bony shelves, which

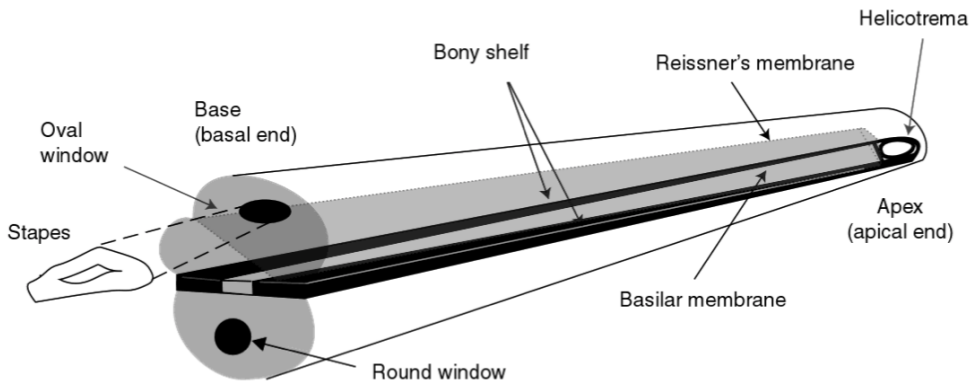

Figure 4: Structure of the cochlea as an opened tube instead of the authentic spiral. Adapted from [6].

have the basilar membrane between them [8]. Helicotrema is an opening at the other end of the cochlea, that connects the liquid between the two compartments. When the stapes moves, it presses against the oval window and pressure propagates in the liquid reaching the round window. This propagation displaces the basilar membrane and causes it to vibrate. The distance of the vibrating point of the membrane to the stapes determines the frequency of the sound. The longer the distance, the lower is the frequency.

On the basilar membrane lies also the organ of Corti. It consists of outer and inner hair cells, which are responsible for converting the vibrations of basilar membrane into neural impulses. There are up to five rows of outer hair cells and one row of inner hair cells evenly distributed on the organ of Corti. Each hair cell has stereocilia on it. They are tiny filaments that bend when the basilar membrane vibrates. Inner hair cells transform the vibrations into neural activity for auditory nerves, while the outer hair cells serve as active "amplifiers" of the mechanical motion. [6]

2.3.2 Human hearing

Humans are able to hear a wide range of sounds from quiet to loud and low to high. A healthy and relatively young person is able to hear frequencies in the *audible range* from 20 Hz to 20000 Hz, but intense enough sounds that are even lower or higher can also be heard. Sounds lower than 20 Hz are called *infrasound* and higher than 20 kHz are called *ultrasound*.

Some common sound pressure levels are presented in fig. 5.

The threshold of hearing is defined to be 0 dB, corresponding to a reference pressure $p_0 = 20$ μPa in air, when 1 kHz pure tone is just noticeably heard. The upper limit of hearing is about 130 dB, after which significant pain is felt and severe hearing loss is possible. The threshold of hearing is not the same throughout the audible frequency range [6]. Also, the hearing sensitivity to different frequencies is dependent on the sound pressure level of the sound. The equal loudness curves for pure tones

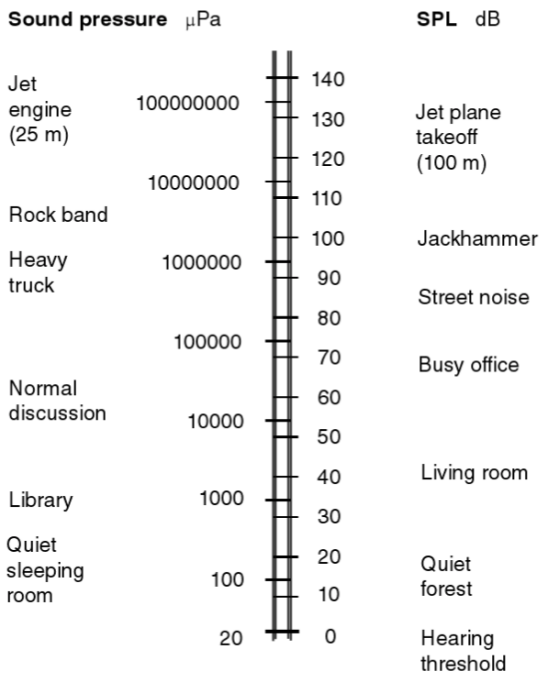

Figure 5: Typical sound pressure levels of different sound events. Adapted from [6].

were defined by Robinson and Dadson in 1956 [9]. These contours also include the minimum audible level for the whole audible range. An equal loudness level is the level that a human perceives as equally loud for a 1 kHz pure tone. The contours are presented in fig. 6.

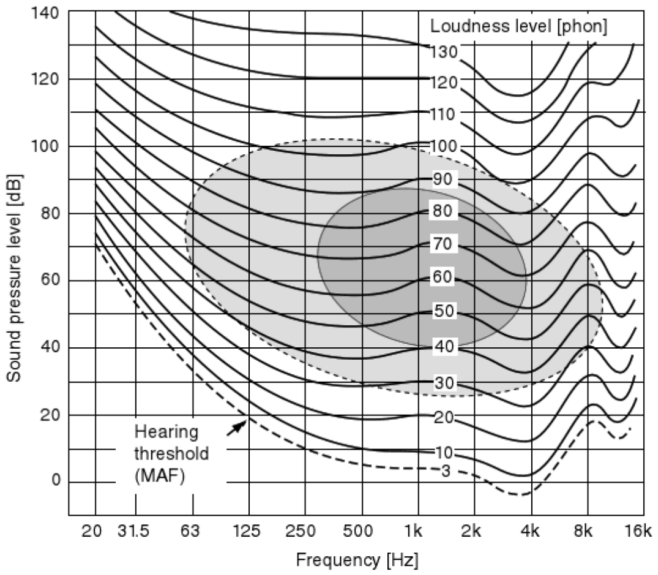

Figure 6: Equal loudness contours in phon-units on a frequency-SPL chart. The dashed line is the hearing threshold measured in Minimal Audible Field (MAF). Adapted from [6].

3 Sound in liquids and solids

Similar to sound propagation in air, the sound waves travel through liquids as longitudinal waves because both of them are fluids. The basic wave equations and mass-spring vibrational equivalences hold true in both media. In addition there are some special considerations to take into account with sound in liquids. This chapter discusses those divergences.

3.1 Basic liquid acoustics

Let us consider water as the initial point of interest regarding sound in liquids. The speed of sound in water c_w is given by

$$c_w = \sqrt{\frac{K}{\rho_w}}, \tag{14}$$

where K is the reciprocal of compressibility and ρ_w the density of water [10]. This approximates to $c_w = 1500$ m/s depending on the water temperature [7]. In sea water, the salinity affects sound velocity. An empirical expression in the temperature range $0 - 20°\text{C}$ and pressure range $10^5 - 10^7$ Pa of the velocity is

$$c_w = 1490 + 3.6\Delta T + 1.6 \times 10^{-6} P_s + 1.3\Delta S \text{ m s}^{-1}, \tag{15}$$

where ΔT is the absolute zero temperature, P is the absolute static pressure in Pa and ΔS an expression for salinity.

A major difference between liquids and gases are their compressibility. Liquids are far less compressible, due to the molecules being closer to each other compared to gases. This entails the influence of intermolecular repulsion. The bulk modulus of any liquid depends mainly on the type of the liquid, temperature and hydrostatic pressure. Generally, the difference between isothermal and adiabatic bulk moduli is minute (less than 1%). This applies to homogenous fluids. The compressibility as well as speed of sound of a liquid, is notifiably changed with liquids that contain gas bubbles. The volumetric strain that would normally be produced is relieved to the bubbles because of the relatively large compressibility of small gas bubbles compared to the liquid's compressibility [4]. The effect of gas bubbles in a liquid is discussed in detail in section 3.2.

Typically, sound is transmitted in water for a wide frequency range of $2 - 50000$ Hz. Thus, sound is also transmitted outside of the audible range in infrasound (< 20 Hz) and ultrasound (> 20000 Hz). If we consider a spherical sound wave in water without any dissipation of energy, the sound intensity I is given by

$$I = \frac{Pe^{-\alpha r}}{4\pi r^2}, \tag{16}$$

where P is the power output, r is radius from the source and $\alpha = 2\mu k^2/3\rho c$. Here $k = 2\pi/\lambda$, ρ is the density, c is the speed of sound, λ the wavelength and μ describes the viscosity, which for water is $\mu = 0.0114$. [3]

In water, the human hearing also behaves a bit differently. The reference of sound pressure level (SPL) in water is 1 μPa at 1 kHz frequency [11]. In addition, the equal loudness curves in water have been measured. Oimatsu *et al.* [12] were able to define the frequency-dependent minimum audible level and equal loudness levels at 122 dB and 142 dB, as well as the relation of loudness between water and air. The results are presented in fig. 7.

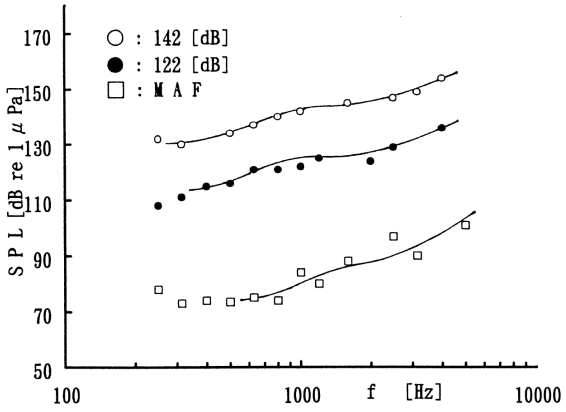

(a) Equal loudness curves in water for 122 dB and 142 dB as well as the minimum audible level.

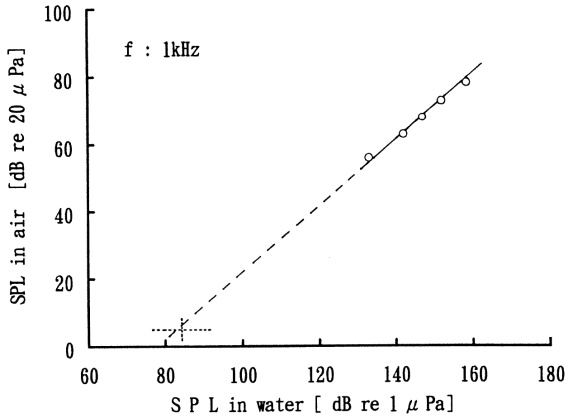

(b) Ratio of sound pressure level in water compared to air by perceived equal loudness.

Figure 7: The equal loudness curves in water (a) and ratio of sound pressure level in water compared to air at frequency of 1 kHz (b). Adapted from [12].

3.2 Loss mechanisms in liquids

3.2.1 Classical absorption

In all fluids, there are two types of classical losses: viscous losses and heat conduction. These phenomena equalize local differences of temperature and velocity and thereby dissipate acoustical energy. The viscosity η of a fluid describes the internal friction of the medium. With a sound wave, there are local variations of temperature and velocity, where molecular-kinetic friction occur. The attenuation of a sound wave is determined by the energy loss caused by internal friction proportional to $\eta\nu^2$ and that is referred to the transmitted energy which is proportional to $\rho\nu^2$. Here ν is the particle velocity and ρ the density of the fluid. The kinematic viscosity term

η/ρ then describes the sound attenuation caused by the friction. For a plane wave travelling in x-direction, the damping is exponential by $e^{-\alpha x}$, where α is similar as in equation 16. [13]

Heat conduction on the other hand, describes diffusion of the kinetic energy, when heat flows from compressed areas to uncompressed ones. Its' losses are in the same order of magnitude with the viscous losses and they are also proportional to $k^2 = (2\pi/\lambda)^2$ (in α). [13]

The classical absorption increases proportionally to the square of the frequency. If only classical absorption is present, the term α/f^2 is constant and it is typically considered as the characteristic classical attenuation. Generally considering and neglecting inhomogenities such as temperature and density fluctuations, sound is less absorbed in bare liquids than in air. For example, a 1 kHz tone plane wave is attenuated by 1 dB at a distance of 10000 km in water but at only 5 km distance in air. [13]

The loss mechanisms described above set the lower limit for losses in liquids and can be taken as the reference level of losses in practical applications. Molecular sound absorption is also the most important source of high attenuation in bare liquids. [13]

3.2.2 Molecular absorption

In addition to the classical absorption of viscosity and heat conduction, molecular absorption is likewise present in liquids. Molecular absorption means that if a fluid is suddenly compressed by an amount, the energy is stored in translational kinetic energy, but also in the rotation of individual atoms in the molecule or oscillations of the atoms with respect to each other. A sudden increase of energy excites the internal degrees of freedom of the molecule. [13]

On the contrary to the rapid energy change, the internal oscillations build up gradually at the expense of rotational and translational energy. The period that the energy increase of the oscillations require is called relaxation time. During the relaxation, different forms of energy reach thermal equilibrium [13]. If the period of the sound wave is greater than the relaxation time, losses occur because the pressure does not reach its' maximum before it is in the decreasing phase. The contrast of rapid energy change to relaxation is presented in fig. 8.

In liquids also other kids of relaxation occurs by ordered and non-ordered domains of a few molecular diameters. A dynamic equilibrium exists between the domains and their establishment is delayed as a function of pressure and temperature. The frequency of this structural relaxation is in the order of magnitude of 100 GHz. In acoustical frequencies, the result is absorption proportional to the square of the frequency, similar to classical absorption. Additional lower frequency relaxation occurs, when certain electrolytes dissociate incompletely in the liquid. [13]

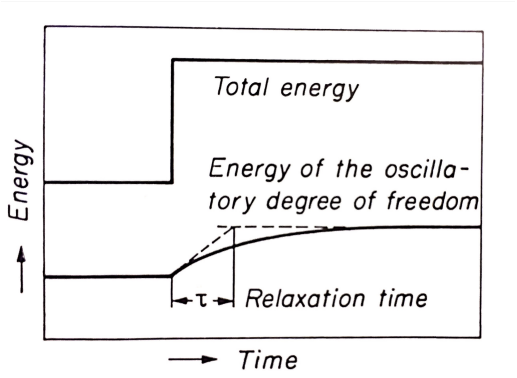

Figure 8: The relaxation time of atom oscillations compared to rapid total energy. Adapted from [13].

3.2.3 Losses by gas bubbles

While solid and liquid particles in gases produce no significant absorption, gas bubbles in liquids on the other hand are a notable source of absorption. A contained gas bubble is an elastic volume and with the oscillating liquid mass acts as a spherical radiator equal to the diameter of the bubble [13]. The resonant frequency is then inversely proportional to the diameter of the bubble [4]. A sound wave drives the oscillating system into forced vibration. Energy from the sound wave is removed by the pulsating bubble and because of heat conduction. This happens because the volume transformation process is polytropic [13].

3.2.4 Losses by presence of walls

Sound propagating in a tube is exposed to additional losses due to a viscous boundary layer between the fluid and the tube. It means that there is a layer of internal friction beside the tube wall. At an acoustically rigid wall, the normal component of velocity dissapears and the maximal value is reached again at 1/4 wavelength distance from the wall. The thickness of the boundary layer is able to be characterized by the viscosity wavelength

$$\lambda_v = 2\pi\left(\frac{2\eta}{\omega\rho}\right)^{1/2}, \tag{17}$$

where η is the dynamic viscosity, and ρ the density of the medium. The attenuation constant of a cylinder tube due to viscous boundary layer is

$$\alpha = 2.7 \times 10^{-2}\frac{f^{1/2}}{R}, \tag{18}$$

where f is the frequency and R the tube radius (in cm). For example, for a tube of

$R = 1.2$ cm, the attenuation is about $\alpha = 0.7$ db/m at 1 kHz. The effect is significant at many meters long tubes. [13]

3.2.5 Acoustic cavitation

Gas bubbles can also be generated in liquids through a process called acoustic cavitation. In the negative pressure phase (antinode) of an intense sound wave a bubble is formed. In the positive phase the bubble is contracted, but in a rectified diffusion process over several periods the bubble grows out from the sound field. This is called gaseous cavitation. [13]

Totally degased and purified liquids require a very high amplitude underpressure before cavitation occurs and it is referred to as hard, pure or vaporous cavitation. The threshold of cavitation is frequency dependent and it depends also on the gas content of the liquid [13]. The cavitation threshold of air dissolved in water is presented in fig. 9. Cavitation also limits the power output of an underwater loudspeaker. In the rarefaction phase at the diaphragm, cavitation can occur, when the pressure rarefaction pressure is near zero. Cavitation effects can be reduced by a relatively high static pressure of the liquid [3].

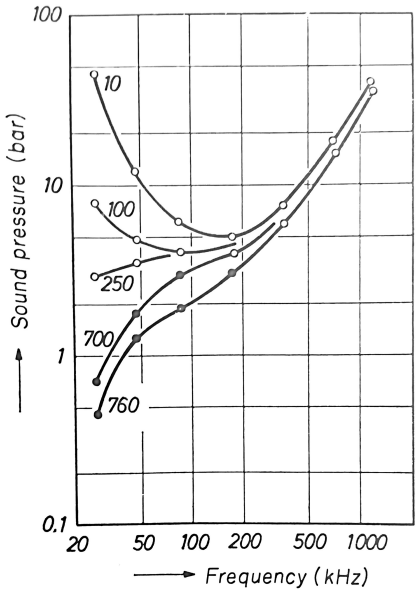

Figure 9: The sound pressure threshold for acoustic cavitation with different air saturation pressures in Torr-unit as a measure of air content in water. Solid dotted lines indicate gaseous cavitation and hollow dotted lines are vaporous cavitation. Adapted from [13].

Another interesting phenomenon concerning cavitation is sonoluminescence. In sonoluminescence, the cavitation bubbles implode and produce very high pressures of more than 10^9 Pa. The temperature also becomes high, for example up to 5000°C in argon at 20 kHz [14]. At the moment of implosion, the bubbles emit flashes of visible

light originating solely to thermal effects. Sonoluminescense was first discovered by Frentzel and Schultes [15] in 1934.

3.3 Sound in solids

Sound in solids behave differently compared to fluids. In addition to the longitudinal waves such as the waves in fluids, solids are able to propagate transverse waves. Transverse waves are particle oscillations in the normal direction compared to the direction of propagation. Elastic properties of solids are characterized by four constants, modulus of compressibility K, shear modulus G, modulus of elasticity E, which is also known as *Young's modulus* and Poisson's ratio μ. Each constant is related to any other one by two of the other constants [13]. E.g. for G expressed by E and μ it is

$$G = \frac{E}{2(1+\mu)}. \tag{19}$$

Solids that extend infinitely to all directions are able to carry two types of sound waves: compressional (longitudinal) and shear (transverse) waves. They are able to propagate in plane, spherical or cylindrical waves. Longitudinal propagation speed is given by

$$c_l = \sqrt{\frac{E(1-\mu)}{\rho(1+\mu)(1-2\mu)}}, \tag{20}$$

and the transverse speed is given by

$$c_t = \sqrt{\frac{E(1-\mu)}{2\rho(1+\mu)}}. \tag{21}$$

Longitudinal waves have always a higher propagation speed than transverse waves. Finite or semi finite solids are able to have even more waveforms such as extensional, torsional and flexural waves. The wavetypes are presented in fig. 10.

The different waveforms all have their unique sound velocity, which is defined by the solid body type. Common examples of these bodies are rods, beams, plates and shells. When sound propagates in different velocities across a body, *dispersion* occurs [16]. Dispersion means that sound propagates with different velocities for different frequencies. It is also related to the concept of *phase velocity*, which is the rate at which the phase propagates in a medium on a certain frequency component. Phase velocity is the quotient of wavelength and time period

$$c_p = \frac{\lambda}{T}. \tag{22}$$

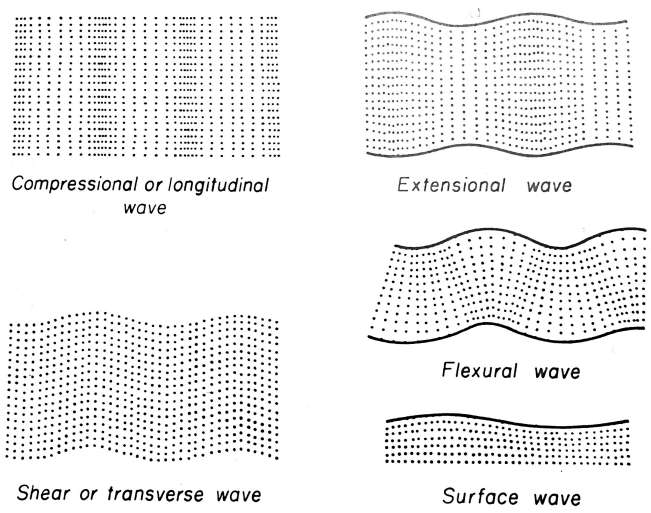

Figure 10: Different wave types in finite or semi-infinite solid bodies. Adapted from [13].

Solids also have *Rayleigh waves*, which are surface waves of solids without any waves inside of the solid body. Rayleigh waves only exist with bodies that are large in comparison with the sound wavelength. Both transverse and longitudinal components occur and the wavy surface is similar to the extensional wave in fig. 10. [13]

Some solid materials such as certain polymers show *viscoelastic* properties. It means that they have both viscous and elastic behaviour under deformation. When shear stress is applied, the viscoelastic materials resist the flow and strain linearly because of the viscosity. At the same time, they do show strain under the stress and try to return to their original state after the stress is removed. [17]

4 Piezoelectric transducers

4.1 Basics of piezoelectricity

Piezoelectric effect occurs, when piezoelectric crystal material is deformed. The crystal also produces an electric polarity as a mechanical force is applied to the material. This is known as the direct effect. In reverse, the crystal material is deformed in an electric field. This phenomenon is known as the converse effect. [18]

In their basic function in small electrical fields and deformations, piezoelectric materials have a structural bias and are in a manner "one-way". Thus, the piezoelectric materials function linearly: when the material is compressed, it gives a certain electrical field and when the material is decompressed, it will emit an opposing field [18]. The linear behavior of the piezoelectric crystals distinguish them from electrostrictive materials. The non-linear electrostrictive behavior, that occurs in all dielectric materials, can also be observed in piezoelectric materials at high electric fields [19]. The strains versus electrical fields of piezoelectric and electrostrictive materials are presented in fig. 11.

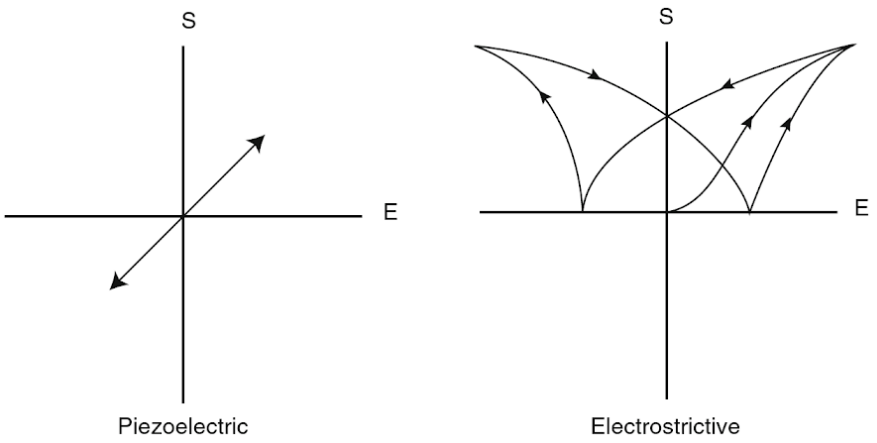

Figure 11: Strain compared against electric field of piezoelectric and electrostrictive materials. The electrostrictive materials behaves non-linearly compared to piezoelectric ones. Adapted from [19].

Piezoelectricity may only occur within crystal structures which have no center of symmetry. There are also polycrystalline piezoelectric materials, which consist of piezoelectric crystallites that are randomly oriented. They present no observable piezoelectric effect as the reaction of individual crystallites cancel. The first discovered piezoelectric materials were quartz, Rochelle salt, ammonium dihydrogen phophate (ADP), and lithium sulfate. The pioneering work with piezoelectricity was done by brothers Pierre and Jacques Curie in the 1880's. They were able to verify the direct and converse effect and cut quartz crystals to polarize them in certain directions. They could produce the *longitudinal effect* by compressing the crystal parallel to the

polarizing direction and the *transverse effect* by perpendicular compression to the polarization. [19]

Non-piezoelectric and barely electrostrictive materials can also be externally polarized by a strong and stable electric field. In practical use, the phenomenon is large enough solely in ferroelectric materials. The strong external electric field guides electric dipoles of the material into approximately the same orientation and makes the bar longer. In weak and arbitrarily directed bias fields the mechanical response of a bar of electrostrictive material is nonlinear, because it lacks proportionality to the electric field. If another alternating field is induced in superposition to the biasing field, the bar of material is able to oscillate around the fixed static strain in an approximately linear manner [19]. This close to linear electrostrictive phenomenon is visualized in fig. 12.

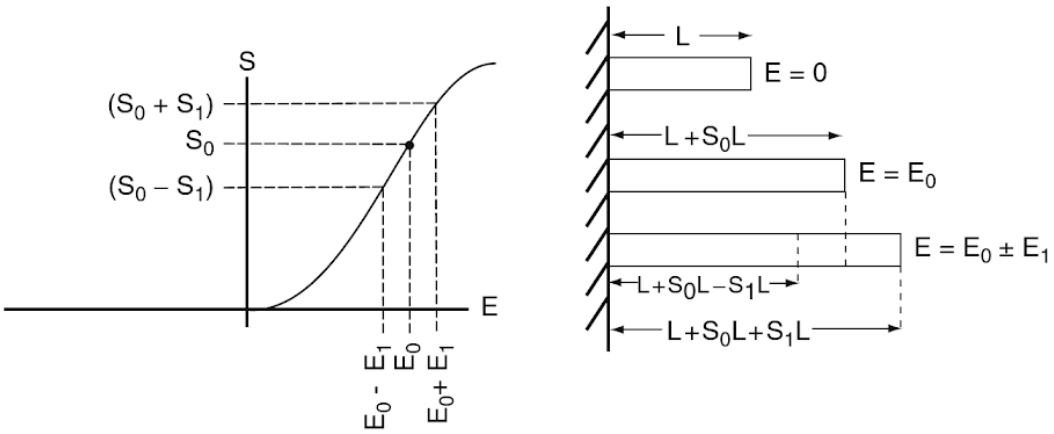

Figure 12: On the left side figure, the strain S_0 is related to the static bias field E_0, while the strain S_1 depends approximately linearly of the alternating field E_1. On the right side figure the impact of these fields are considered regarding the change in length L of the bar made out of electrostrictive material. Adapted from [19].

4.2 Brief theory of piezoelectricity

The fundamental theory behind piezoelectricity begins with understanding the relation between electrical field E, and mechanical stress X. When a piezoelectric crystal is in an electric field, also an electric polarization P emerges. By varying the stress and electric field by tiny amounts dX and dE, the change in energy is expressed as the differential $dU = P\ dE - x\ dX$. As a reversible process it can be expressed as

$$\left(\frac{\partial P}{\partial X}\right)_E = -\left(\frac{\partial d}{\partial E}\right)_X, \tag{23}$$

and over a large range of different crystals and amount of compression, the relation is linearly proportional, leading to

$$\frac{\partial P}{\partial X} = -\delta, \tag{24}$$

where δ is the piezoelectric strain constant. Equation 24 describes the direct effect and the term $\partial d/\partial E$ describes the converse effect with a reversed sign of δ. [18]

If we assume isothermal conditions and apply the elementary piezoelectric strain equations as in [18], we are able to derive the fundamental piezoelectric equations concerning the strain and field

$$\frac{\partial \xi}{\partial x_h} = \sum_{i=1}^{6} c_{hi}^{E} x_i + \sum_{m=1}^{3} e_{mh} E_m = -(X_h), \tag{25}$$

$$\frac{\partial \xi}{\partial E_m} = \sum_{k=1}^{3} \eta''_{km} E_k + \sum_{h=1}^{6} e_{mh} x_h = P_m, \tag{26}$$

where eq. 25 describes the converse effect and eq. 26 the direct effect. The e_{mh} terms are the piezoelectric stress coefficients or *Voigt's piezoelectric constants*. Term ξ, describes the *second thermodynamic potential*, strain, c the elastic stiffness and η the dielectric properties of the crystal material. Regarding the external stresses, the fundamental equations can be derived to

$$\frac{\partial \zeta}{\partial X_h} = \sum_{i=1}^{6} s_{hi}^{E} X_i - \sum_{m=1}^{3} d_{mh} E_m = -x_h, \tag{27}$$

$$\frac{\partial \zeta}{\partial E_m} = \sum_{k=1}^{3} \eta'_{km} E_k - \sum_{h=1}^{6} d_{mh} X_h = P_m, \tag{28}$$

where again eq. 27 describes the converse effect and eq. 28 the direct effect. Now the terms d_{mh} are the piezoelectric strain coefficients, or *Voigt's piezoelectric moduli*. η' and η'' are the free and clamped susceptibilities, s_{hi} is the elastic compliance and ζ the *second thermodynamic potential*, stress. [18]

In the above equations, the term X_h expresses total stress that consists of two components: the externally applied stress producing strain in the circumstance $E = 0$ and the piezoelectrically induced stress by E. In other words, the piezoelectrical body stress is equal and opposite to the external stress and it ought to be added to the mechanical stress causing the first term in the equation 25. Otherwise the strain constant would not hold in the applied field. If the field and strain are pre-assigned, the total stress X_h will be

$$X_h = \sum_{i=1}^{6} c_{hi}^{E} x_i + \sum_{m=1}^{3} e_{mh} E_m = (X_h) + 2 \sum_{m=1}^{3} e_{mh} E_m. \tag{29}$$

This distinction between external stress vs. the sum of two stresses has to be borne in mind in order to not confuse the external and and internal phenomena with each other. [18]

By reducing the subscripts and their sums from the equations, as well as further on ignoring the thermal variations, the principles of these formulae can be articulated as

$$\xi = \frac{1}{2}c^E x^2 + \frac{1}{2}\eta'' E^2 + eEx, \tag{30}$$

$$\zeta = \frac{1}{2}s^E X^2 + \frac{1}{2}\eta' E^2 - dEX. \tag{31}$$

4.3 Flexural piezo transducers

There are several types of piezo transducers such as spherical, ring, piston transmission, flextensional, and modal transducers [18]. This section depicts the principles of flexural transducers, the type of piezo that is used in the experimental part of this work in section 6. Flexural piezos have been found practical both as underwater sound projectors as well as for capturing underwater sound.

4.3.1 Flexural transducers in general

Flexural transducers operate in in-extensional bending modes. This means that the neutral plane length does not vary, but the transducer bends instead. The piezo driver extends on the other side and contracts from the opposite side. This phenomenon is presented in fig. 13.

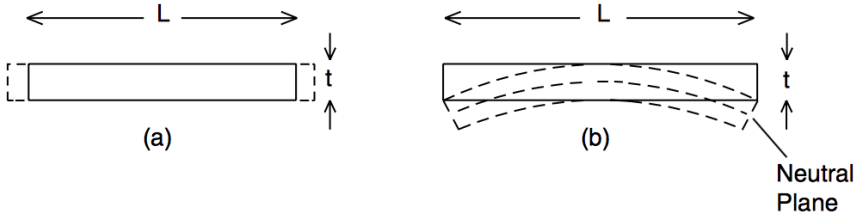

Figure 13: Flextensional piezo movement. Neutral plane length is constant and the transducer is bending. Adapted from [19].

The contraction and expansion of the opposite sides leads then to zero net extension. For the non-clamped bars of fig. 13, the fundamental resonance frequencies of longitudinal extension f_r and bending inextension f_i are given by

$$f_r = \frac{c}{2L}, \tag{32}$$

$$f_i \approx \frac{tc}{L}, \tag{33}$$

which lead to

$$f_i \approx \frac{2f_r t}{L}, \tag{34}$$

where c is the sound velocity and t is the thickness of the bar.

Bender mode transducers are well suited for low frequency applications, where large drivers would not be applicable. This is due to the quality of low resonant frequency with a large and thin driver. If the driver bar is thick and has $t = L/2$, the resonant frequencies f_i and f_r would be approximately the same. On the other hand a thin bar with $t = L/20$, the resonance f_i would be a decade lower than f_r. [19]

The thin and long qualities of bender mode transducers make them convenient for audible range applications. Modelling and analysis of these flexural transducers is more challenging than conventional longitudinal mode based transducers despite of the fact that their geometries are fairly simple. [19]

4.3.2 Bender disc piezo transducers

Flexural transducer discs are excited by the planar radial mode. With a bender disc that has its edges clamped, the fundamental resonance frequency for a diameter D and thickness t is

$$f_r = \Big[1.868c/(1-\sigma^2)^{1/2}\Big]t/D, \tag{35}$$

which approximates to $f_r = 2ct/D^2$ when Poisson's ratio is $\sigma \approx 0.33$. If the edge is only simply supported, the fundamental frequency is then

$$f_r = \Big[0.932c/(1-\sigma^2)^{1/2}\Big]t/D, \tag{36}$$

approximating to ct/D^2 with the same Poisson's ratio. Thus, the fundamental resonance is only half compared to the clamped edge disc. When the disc is placed into water, it is mechanically loaded and the mass reduces the resonant frequency according to

$$f_w = \frac{f_r}{\Big[1 + 0.75(a/t)(\rho_0/\rho)\Big]^{1/2}}, \tag{37}$$

where t and a are the thickness and radius of the disc and ρ_0 and ρ are the densities of water and the disc. [20]

The common designs for flexural piezo discs are trilaminar and dual bilaminar bender discs, which are presented in fig. 14.

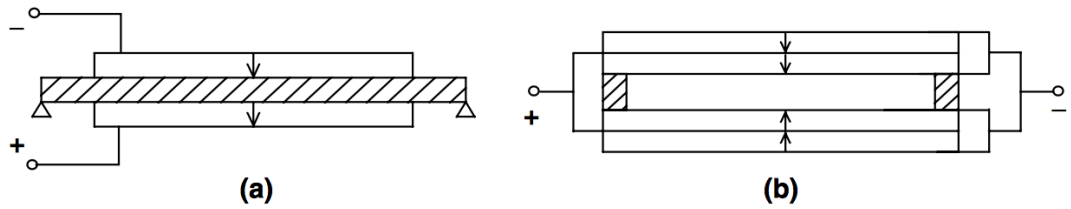

Figure 14: Designs for (a) trilaminar and (b) dual bilaminar discs. Adapted from [19].

In the dual bilaminar design, the inner support ring is usually axially stiff and radially compliant. This way the disc is can fulfill the simple support boundary condition approximately. Design formulae have also been developed to estimate the dual bilaminar discs performance. In water the ratio of resonant frequencies in water and air is given by

$$\frac{f_r}{f_w} = (1 + 0.10a/t)^{1/2}. \tag{38}$$

One of the deficiencies of bender discs is the piezoelectric materials' low tensile stress limit in hydrostatic pressure. Therefore, discs with an inactive metal core have been designed. The largest flexural piezo disc that can be manufactured is approximately 18 cm in diameter. It also has maximum coupling effect when the outermost discs and the inactive metal layer of a trilaminar disc have equal thicknesses. [19]

The underwater loudspeaker in the measurement setup described in section 6 is based on flexural type piezo transducer.

4.4 Hydrophones

A hydrophone is an electromechanical transducer, that is able to transform mechanical vibrations of fluids into electrical signals. They are especially designed to operate in liquids and even more specifically, in water. In acoustics, a hydrophone in water is the equivalent of a microphone in air.

Hydrophones pick up changes in pressure in water and their output is a voltage proportional to the pressure. Hydrophones are able to be built to be more robust than microphones because for the same intensity in water the pressure is 600 times higher and particle velocity about 600 times lower compared to air. Hydrophones are able to capture sound from air, but they are very sensitive due to the mismatch

between acoustical impedance of air and the transducer. Piezoelectric microphones also exist. Hydrophones are typically based on piezoelectricity, such as quartz crystal and Rochelle salt crystal materials. They are also able to be built based on magnetostrictive or capacitive principles. [3]

5 Sound propagation in a fluid-filled tube

Typically, sound propagation in tubes is something to be prevented. This is the case for example in ventilation ducts in buildings, where the noise needs to be attenuated. It is more rare that good sound transmission is desired in a tube, such as in the scope of this work. One early example of sound transmission through tubes was in marine ships, where transmit commands were passed through several meters long tubes from the bridge to the engine room [13]. This chapter discusses the characteristic properties of sound transmission through liquid filled tubes.

5.1 Sound fields in rigid wall waveguides

In arbitrarily large volumes of fluids, the sound waves are propagating freely to every direction and the energy is spread without limits in cylindrical wavefronts. However, in tubes the sound energy is contained to follow the tube path and the sound is only able to propagate as a plane wave [4]. The wavelengths λ, that are larger than the cross-sectional diameter of the tube, can solely propagate as a plane wave. In a rigid-walled uniform tube with a lossless medium, the plane wave will propagate without attenuation.

This type of one dimensional wave propagation can be described with a *wave equation*

$$\frac{\partial^2 y}{\partial t^2} = c^2 \frac{\partial^2 y}{\partial x^2}, \tag{39}$$

with the solution

$$y(t, x) = g_1(ct - x) + g_2(ct + x), \tag{40}$$

where y is the physical variable, t is time, x is the observation point and c is the sound velocity. g_1 and g_2 are two waveforms that are travelling in negative and positive directions [6].

The plane wave in a tube is entirely described by the sound pressure p and volume velocity q $[m^3/s]$. They have a linear dependence by the *acoustic impedance* Z_a by

$$p = Z_a q. \tag{41}$$

Acoustic impedance of a medium is given by it's physical properties $Z_a = \rho c/A$, where ρ is the density of the medium and A the cross-sectional area of the tube [6]. There are discontinuities in the acoustic impedance if any of the parameters in the tube change. These impedance mismatches cause reflections in the travelling plane

wave. The reflection coefficient R is relationship between the two impedances Z_2 and Z_1

$$R = \frac{Z_2 - Z_1}{Z_2 + Z_1}. \tag{42}$$

The transmission coefficient T is given by $T = 1 - R$. This phenomenon is presented in figure 15.

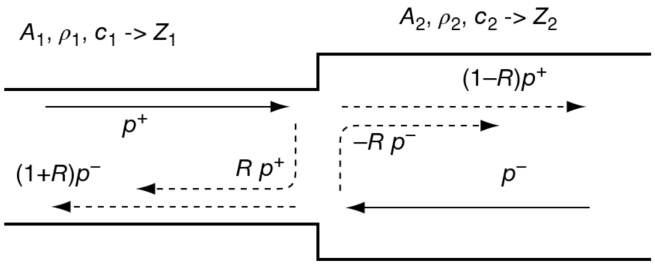

Figure 15: Plane wave reflection and transmission at an impedance discontinuity. p^+ is the pressure wave travelling from left to right. Adapted from [6].

When reflections occur in the terminations of a tube, also standing waves are formed. The natural frequencies, also called *modes* are dependent on whether the ends of the tube are closed or open, in other words rigid or non-rigid respectively. Non-rigid termination could have frequency dependent complex impedance with non-zero resistance [4]. The axial modal behavior in open and closed-end tubes is presented in fig. 16.

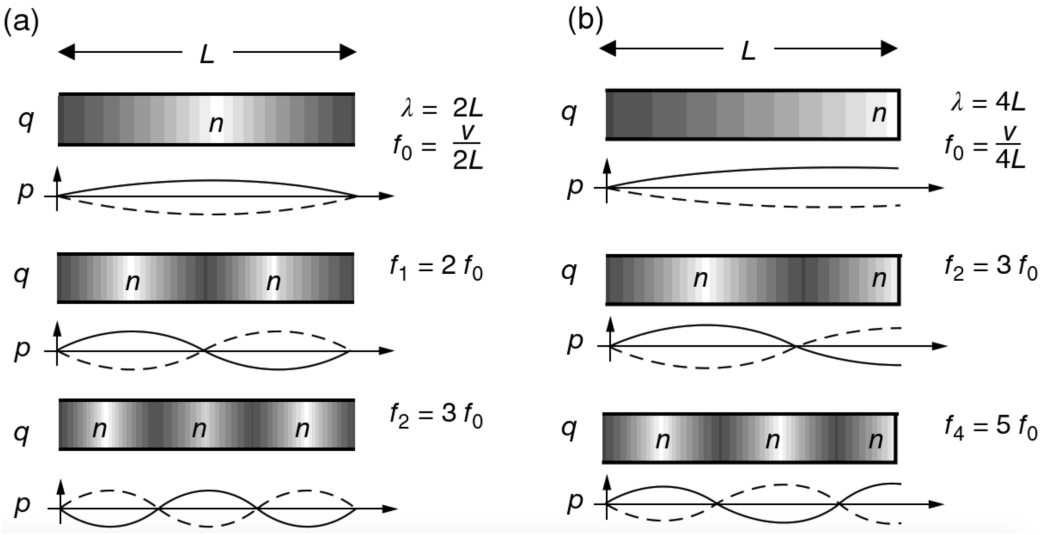

Figure 16: Modal behavior in tubes with open ends (a) and one end closed (b). Letter n shows the minima of particle velocity. Adapted from [8].

The figure shows that open ends always have pressure minima, and closed ends a pressure maxima. Vice versa there is always a maximum of particle velocity in open

ends and minimum in closed ends. The lowest modal wavelength that a tube with both ends closed or open is able to contain, is always double of the tube length L. In other words, the lowest standing wave frequency is half of what the tube can contain. Free vibrations are thus given by

$$f_n = \frac{nc}{2L}, \tag{43}$$

where n is the order of the mode and c is the speed of sound. [4]

On the other hand, the lowest modes in a tube with opposite terminations are four times the tube length. Consequently, only a quarter of the lowest mode wavelength "fits" into the tube.

5.2 Sound fields in cylindrical waveguides

Waveguides with a circular cross section can be analyzed in cylindrical coordinates. The coordinate system is presented in fig. 17.

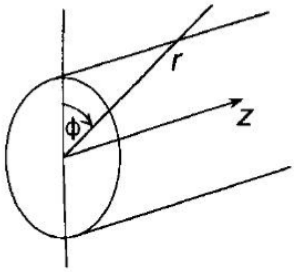

Figure 17: Cylindrical coordinate system. Here r is the radial distance, Z axial distance and ϕ is the radial angle. Adapted from [4].

The Helmholtz form of cylindrical waveguide equation is

$$\frac{\partial^2 p}{\partial r^2} + \frac{1}{r}\frac{\partial p}{\partial r} + \frac{1}{r^2}\frac{\partial^2 p}{\partial \phi^2} + k^2 p = 0, \tag{44}$$

where p is the pressure inside the waveguide, r and ϕ the radial coordinates and k the wave number. The plane wave modal solutions with a rigid wall condition at the surface $r = a$ are

$$p_{mn}(r, \phi) = A_{mn} J_m(nr/a) \begin{matrix}\cos \\ \sin\end{matrix} (m\phi), \tag{45}$$

where $J_m(nr/a)$ is a Bessel function of order m. The Bessel function series of order m are given by

$$J_m(x) = \frac{(1/2x)^m}{m!} - \frac{(1/2x)^{m+2}}{1!(m+1)!} + \frac{(1/2x)^{m+4}}{2!(m+2)!} + ... \tag{46}$$

A few of the first order Bessel functions are presented in fig. 18.

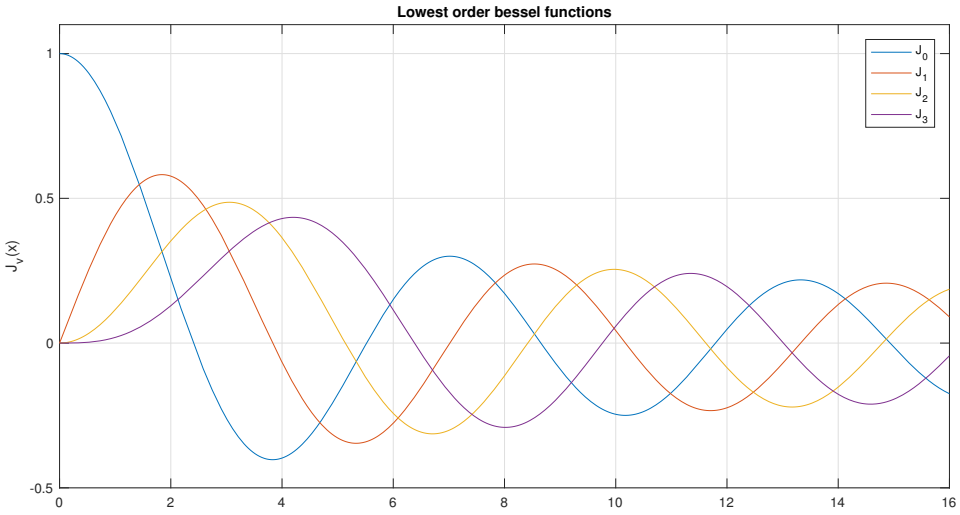

Figure 18: Four lowest order Bessel functions.

The zero radial pressure gradients of the Bessel functions describe the rigid wall boundary condition. On the other hand, at maximum pressure gradients radial particle velocity is at its maximum. The sin and cos -functions of equation 45 describe nodal surfaces at the angular interval π/m, where the circumferential particle velocity is at maximum. Cross-sections of low-order modes with uniform phase in a cylinder are presented in fig. 19.

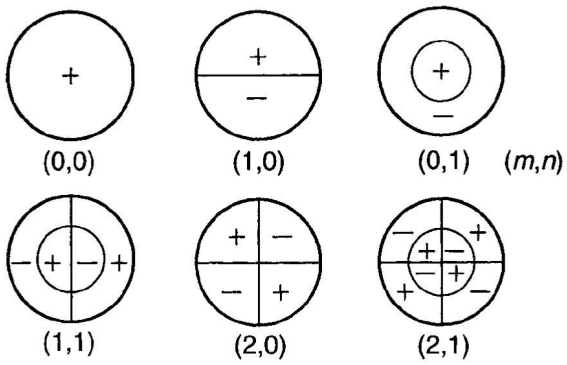

Figure 19: Cross-sections of low-order modes of a cylindrical waveguide. Adapted from [4].

This type of cylindrical waveguide introduces a modal cut-off phenomenon [4]. The lowest cut-off frequency is described as $ka = 1.84$, where k is the wave number $k = 2\pi/\lambda$.

5.3 Tubes with pressure release walls

Section 5.1 describes the sound propagation of fluids in a rigid wall tube. For light gases such as air, many solids such as metals fulfill the condition and the pressure release at walls can be neglected in simple practical applications. In these cases, the intrinsic sound velocity is equal to the phase velocity of the propagating wave. The wavefront can also be assumed to be planar and purely longitudinal [21]. A system that incorporates a fluid inside an elastic shell with pressure release walls, has far more complex wave behaviour [22]. Pure plane waves do not exist in non-rigid waveguides, as the pressure on the wall produces particle displacement normal to the wall. The lowest order mode is called *principal mode*, which usually carries most of the energy. Higher order mode cut-off frequencies are also different than rigid-wall waveguide ones [4].

For liquid-filled elastic tubes, the rigid wall approximation is usually incorrect as the elastic moduli and density of the tube wall and the fluid are typically of equal magnitudes. The inside fluid and outside solid shell form a *coupled system* with complex vibrational modal behaviour. [21]

The vibrational motion of a cylindrical shell can be described by simplified Flügge equations [23]. The equations are thoroughly addressed for example in [24] and they will not be reviewed in the scope of this work. The wave motion in a fluid on the other hand can be described by a linear acoustic equation and solved by Bessel and cosine functions as described in section 5.1. If the radial particle velocities of the tube and liquid are set to be same at the wall, the solutions can be matched to the characteristic equation

$$x_n J_n'(x_n) L_1(y_n) = \eta \Omega^2 J_n(x_n) L_2(y_n), \tag{47}$$

where x_n is the normalized radial wave number in the fluid, y_n is the normalized axial wave number, J_n is the Bessel function of order n, L_1 and L_2 Flügge equations and Ω is the normalized frequency. The subscript n refers to the circumferential distribution $cos(n\phi)$, where ϕ is the cylindrical angle coordinate. Parameter for coupling, η is approximately two times the unit length fluid mass divided by unit length shell mass given by

$$\eta = \frac{\rho_{\text{fluid}}\, a}{\rho_{\text{shell}}\, t} \approx 2 \times \frac{\text{unit length fluid mass}}{\text{unit length shell mass}}, \tag{48}$$

where a is the inner tube radius and t the thickness of the tube. [24]

Equation 47 describes the physical meaning of a tube vibrating *in vacuo* ($L_1(y_n) = 0$) and an acoustic wave in a rigid walled tube ($x_n J_n'(x_n) = 0$). The two vibrations are coupled together by a wave mode dependent coupling coefficient $\eta\Omega^2 J_n(x_n) L_2(y_n)$. When the coupling parameter η is zero, there is no coupling [24]. In other words, this means that when the density of the fluid is minor compared to the density of

the tube, the simple plane wave propagation inside the tube described in section 5.1 is true. This is the case for example with air and most solid materials, but it does not apply to e.g. water based liquids in PVC tubing, where the density ratio $\rho_{\text{water}}/\rho_{\text{shell}} \approx 1/1.4$, which is close to unity (approximately equal density). On the other hand the air-PVC ratio is $\rho_{\text{air}}/\rho_{\text{shell}} \approx 1.2/1400$ which is in the order of 10^3 closer to zero. The density ratio as well as the shell thickness ratio to the tube diameter determines the proportion of energy contained in the fluid or shell type waves [22].

Different modes of free vibrations exist in the cylindrical tube shell, when it is excited by an external force. The types of the shell motion may be flexure, extension or torsion. Different mode types are presented in fig. 20.

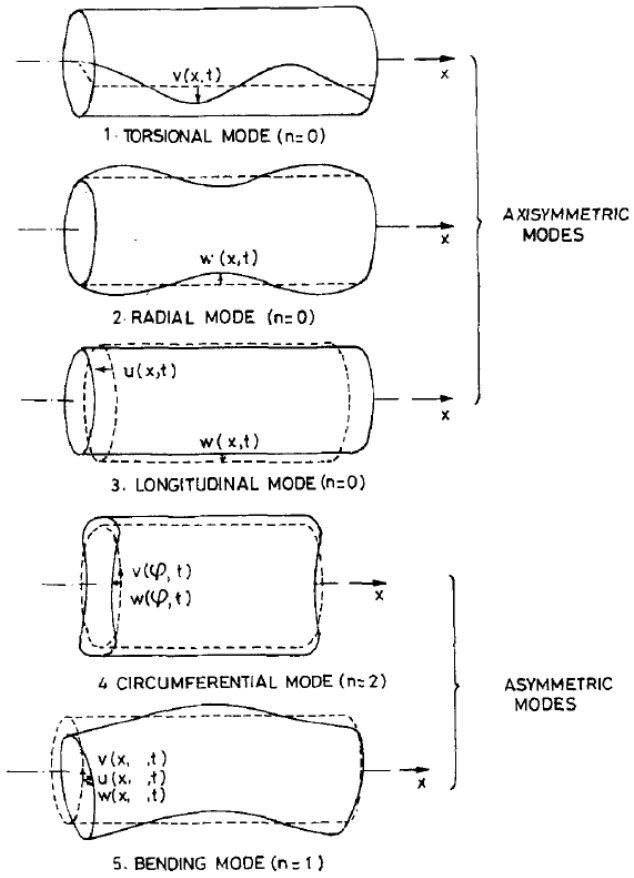

Figure 20: Different types of vibration modes of a cylindrical shell. Adapted from [25]

By looking at figs 19 and 20, we are able to deduce the interaction between plane wave modes and the shell modes. For an arbitrary cross section of the tube and an arbitrary plane wave mode (m, n), we see that the plane wave has regions of over pressure and under pressure. The over pressure areas are pushing the shell outwards and under pressure areas are pulling it inwards. With pressure release walls, the

shell moves according to those pressure changes and causes modal behavior in the tube.

Pavic [26] showed that there are four assumed wave types in the coupled shell and fluid caused by axial forces, torsional shear, transverse shear and bending moment. The longitudinal acoustical waves carry energy both in the fluid and the wall. It was concluded that bending waves only causes small energy flow in the fluid and torsional waves of the shell do not interfere with the fluid. Because the tube and fluid motion are known, the energy flow could be determined from only surface vibrations. The point of interest in the study was in straight tubes.

Xu [27] found that at non-dimensional middle frequencies ($1.0 < \Omega < 2.0$) all of the circumferential mode orders the shell *in vacuo* results in larger effect than the fluid filled shell. When external force is applied, the shell vibrates resonantly with the force meanwhile the fluid's effect is reducing the resonant response. It was found that for all frequencies the transmitted power of bending moment and transverse shear forces are equal.

Feng [24] showed that the different circumferential modes also radiate sound power outwards to the surrounding medium at some of the modes. The radiated sound power is related to the ratio of fluid power and it can be described as transmission loss. No definite relation of radiated sound power to the energy distribution in the system was found. It was concluded that at low frequencies the transmission loss of non-axisymmetric modes is at least 30 dB smaller than axisymmetric breathing modes. The total transmission loss is considerably smaller if any non-axisymmetric modes are excited. Also the radiated sound power varies with the axial distance, because of the distribution of the radial velocity of the tube. Thickness of the shell affects the radiated power at middle and high frequencies.

In the experimental work of Horne and Hansen [28], it was found that viscoelastic tube materials attenuate sound compared to more rigid materials along the axis of the tube. The attenuation at 91.44 cm from the sound source was about 10 dB at 100 Hz and more than 60 dB at >1000 Hz compared between acrylic and rubber/hypalon tubes. The measurements were done with 182.90 cm long water filled tubes of 20 cm in diameter. It was also found that the most attenuation occurs in the materials with lowest elastic shear moduli.

Jacobi [29] also reports energy dissipation and attenuation of several decibels per foot with pressure release walled tubes. The experiment used an automobile radiator hose made of rubber with water inside. The experimentally obtained lowest modal cut-off frequency for the tube of 45 mm in diameter was 26 kHz.

The importance of the type of external excitation to the system is discussed. Many studies [22] [24] [27] [30] found that the point of vibration excitation is important for the behavior of the coupled tube-fluid system. For structural excitation to the tube, most of the energy propagates in the shell and for acoustical excitation to the fluid the energy is primarily in the fluid. At higher frequencies the energy is in the fluid field or in the tube [22].

With fluids inside elastic shells, the phase velocity is slightly slower than the sound velocity [21]. The different scenario originates from the compressibility of the fluid. It has also been found that the distensibility of the tube is more important that the compressibility with thin walled tubes, as water may be considered incompressible [31].

The modes of propagation for elastic wall tubes have been studied also in [32], [33], [34], [35], [36], [37] and [38] with varying concentration on the types of modal behavior. These papers give only a reduced view on the fluid-shell interaction. Many works concentrate on simplified models, such as beams and rods or single-component impedance models.

6 Measurements and results

A series of measurements were done to quantify the ability of a liquid filled elastic tube to propagate sound induced with a piezo transducer. The primary aim of the measurements was to evaluate if it would be possible to transmit sound through viscous liquid filled tubes. The vibrations of the tube were examined in different positions of the liquid-tube system. Also the preconditions given in section 1 should be fulfilled by the measured system so that it would be able to be used in MRI scans.

The different measurements included preliminary testing with small scale piezo components, magnitude response measurements with laser doppler vibrometer and a hydrophone. In addition measurements along the outer surface of the tube and inside of it were carried out to estimate the sound pressure level attenuation.

6.1 Measurement methods

The measurements described in sections 6.2 - 6.5 were conducted with the following equipment:

- Collection of small scale piezo disc components + impedance matching transformer
- Oceaners DRS-8 underwater loudspeaker + impedance matching transformer
- Aquarian audio AS-1 hydrophone & PA-4 preamplifier
- MOTU UltraLite-mk3 audio interface
- Quad 240 Power amplifier
- Polytec OFV 303 Sensor head & OFV 3001 S Vibrometer controller

The measurements were conducted with 1 second long logarithmic sweeps between 20 Hz and 20 kHz with 0.5 seconds of silence in the beginning and end of the sequence. The sampling frequency of the system in all of the measurements was 48 kHz. Impulse responses were calculated as well as the frequency domain magnitude response. The magnitude responses were calculated by Fast Fourier Transform (FFT) with 4096 frequency bins. Also the background noise of the system was recorded. The measurements were processed in Matlab with the exception of the preliminary measurements, which were processed in Fuzzmeasure -software.

The attenuation of sound along the tube length was measured by the decay of sound pressure level L_p by calculating root-mean-square -value (RMS) of the impulse response. The analysis was done in octave bands in 10 octaves according to the ANSI S1.11 standard [39].

The liquids used in the experiment were water and a strongly viscous emulsion containing:

- Water
- Caprylic/Capric Triglyceride
- Isopropyl Palmitate
- Glyceryl Stearate
- Glycerin
- Cetyl Alcohol
- Peg-30 Stearate
- Ceteareth-20
- Ethylhexylglycerin
- Phenoxyethanol

The liquid is a commercially available skin cream. It was chosen to be used by recommendation from a medical doctor, as the liquid should be able to be inserted into a person's ear, possibly even touching the tympanic membrane. It will be referred as *emulsion* in this work. Also measurements with the tubes filled with air were made. The tubing used in the experiments were polyvinyl chloride (PVC) used for example in the food industry. The inner diameter of the tube was $d_1 = 9$ mm and it's thickness was $t_1 = 1.8$ mm except for the measurements in section 6.4, which were $d_2 = 32$ mm and $t_2 = 4$ mm. Densities of the used media and materials are presented in table 1.

Table 1: Densities of sound propagating materials and media.

Medium	Density ρ, kg/m^3
Water	997
Emulsion	952
Air	1.2
Polyvinyl chloride (PVC)	1400

In this work, the speed of sound in both of the liquids is approximated to the speed of sound in water. Obtaining the compressibility of water at 20°C from [40] the speed of sound in water is $c_w = 1485$ m/s by eq. 14. Longitudinal and transverse sound velocities in the PVC tube are calculated by the equations 20 and 21 and by obtaining elastic properties of PVC tube from [41] to be $c_l = 1860$ m/s and $c_t = 980$ m/s.

6.2 Preliminary measurements

A variety of small scale piezo transducers were tested to evaluate their potential to be used in the final application. All of the transducers were flexural type bender disc piezos described in section 4.3.2 with diameters varying from 10 mm to 27 mm. The used PVC tube was 50 cm long.

Filling the tube completely with the strongly viscous emulsion and without any air pockets inside the tube was found to be close to impossible by available practical methods. Several attempts were made to find the practically achievable best result to avoid the additional attenuation by air bubbles (see section 3.2.3). Because the tube was filled by hand with a syringe, the maximum fill length was about 1 m after which the friction of the sliding emulsion column was restricting the emulsion insertion. Adapters were designed and 3D-printed to act as a waveguide and match the diameters of the piezo disc and the tube.

The piezo disc was joined to the adapter at the end of the tube by elastic glue from its edges. The other end was submerged into a container of 400 ml of the cream along with the hydrophone.

The measured magnitude responses of a small scale piezo disc and background noise are presented in fig. 21. The presented small scale piezo is the best performing one of the five measured discs. The level of the piezo disc playback was set to a level where it did not produce detectable harmonic distortion. Each of the piezo discs produced fairly similar results compared to the presented one.

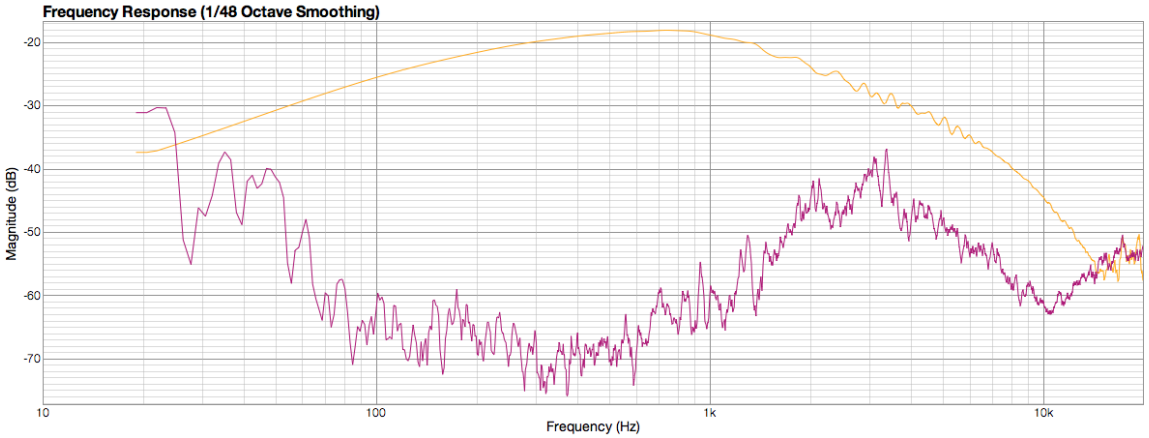

Figure 21: Magnitude responses of the system and background noise in yellow and purple color respectively.

In the measurement, the signal to noise ratio (SNR) at frequencies from 3 kHz to 10 kHz is poor SNR = 10...15 dB. From 10 kHz to 20 kHz, the SNR is approaching 0 dB. Music was also played back and recorded. The recording included a significant amount of audible noise (as expected), but also indicated that only a little amount of sound was propagated through the tube, though it was only 50 cm long. From

the preliminary measurements it was concluded that a more powerful sound source was needed to be able to transmit sound to the desired length of 5-10 m.

6.3 Laser doppler vibrometer measurements

After it was concluded, that the small scale piezo discs would not produce enough output power, an underwater loudspeaker (Oceaners DRS-8) was used in the subsequent measurements. A laser doppler vibrometer was used to measure the system's response. The output of an audio interface handling the analog-to-digital and digital-to-analog conversions was connected to an audio power amplifier. From the audio amplifier the output signal moved forward to the underwater speaker through an impedance matching transformer. That is due to the typically high input impedance of piezo transducers (4000 Ω) compared to the typical output impedance of audio amplifiers (4/8 Ω).

The underwater loudspeaker playback level was set to as high as possible without distorting it. The playback level was kept constant throughout the measurements. The underwater loudspeaker was connected to a conical hard plastic waveguide, whose diameter was linearly diminishing to match the diameter of the tube. The plastic waveguide was pressed firmly against the loudspeaker with an elastic layer of insulating material between them. The tube was connected to the plastic waveguide with a 3D-printed adapter and both the waveguide and tube was filled with liquid. At the other end of the tube was a thin, lightly stretched rubber membrane to block the liquid from leaking out and providing a reflecting surface for the laser.

On the input side was the laser vibrometer with the sensor head connected to it's controller unit. The actual laser was pointed and focused to the rubber membrane on the center axis of the tube. The vibrometer was measuring velocity of the membrane in the axial (longitudinal) direction of the tube. As the tube is open ended, there is a velocity maximum. Bronze dust was used to enhance the reflection from the membrane. The output from the controller unit fed signal to the input of the audio interface, which was analyzed in the computer. A block schematic of the measurement setup is presented in fig. 22.

6.3.1 Air filled tube

The tube lengths of 1 m, 4 m, and 8 m were measured for the air filled tube. Air filled tube was measured to have a reference measurement for the liquid filled tubes. As given in section 5.2, the lowest cutoff-mode for a one dimensional plane wave propagation to exist in a tube can be derived to

$$f_{c,AIR} = 1.84\frac{c}{\pi a} = 22321 \text{ Hz}, \tag{49}$$

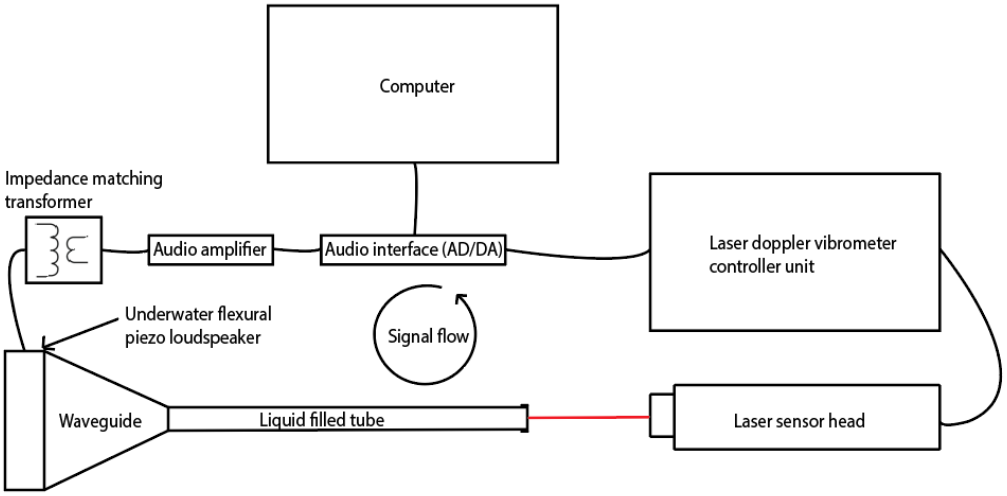

Figure 22: A block schematic of the measurement setup.

when sound velocity in air is 343 m/s. Thus, the whole audible frequency range can be taken into account assuming rigidity of the tube walls. The measured magnitude responses are presented in fig. 23.

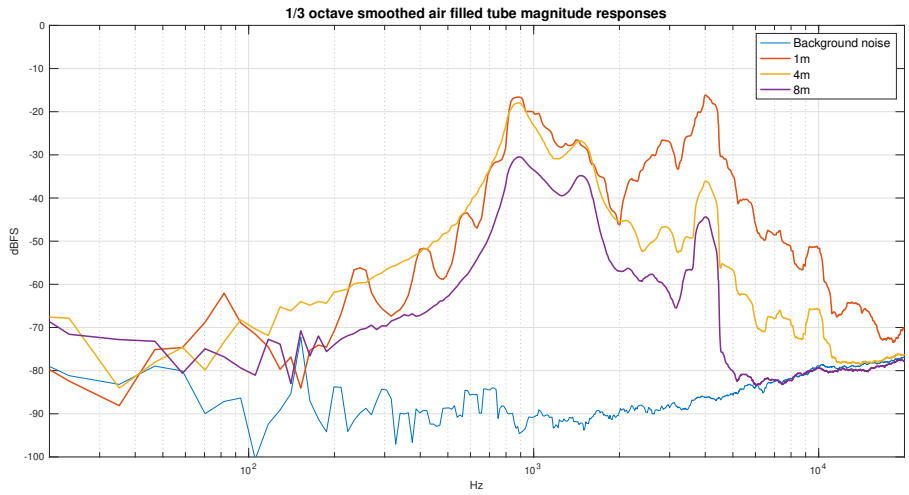

Figure 23: The magnitude responses of air filled tubes of different lengths.

From the air filled tube magnitude responses we see that most of the sound energy lies between 600...5000 Hz. This is mostly due to an impedance mismatch between the underwater loudspeaker and air. Attenuation is seen by the high frequencies and the largest peaks in this frequency range. At 900 Hz peak the attenuation is 14 dB from 1 m to 8 m. At 4 kHz peak the attenuation is 28 dB. High frequencies are attenuated more and at 8m distance the signal hits background noise level from 6 kHz and above. A low-pass characteristic of the system can be seen. As the distances are very short even in terms of one dimensional plane wave propagation assumption,

the attenuation is assumed to occur due to the pressure release effect of the walls. Classical attenuation is not considerable due to the very low viscosity and thermal conductivity of air.

6.3.2 Liquid filled tube

The endpoint velocity of liquid filled 1 m long tubes were also measured. Two variations of liquids were measured. One with the whole tube and waveguide filled with the emulsion and another one which had 95 cm of water and 5 cm of the emulsion at the end of the tube. The mostly water filled tube was measured to evaluate the difference of attenuation between the strongly viscous emulsion and less viscous water. The emulsion was needed to stop the water from flowing out. Figs A1a and A1b in Annex A show the measurement setup.

In water, the lowest cutoff mode according to equation 5.2 would be $f_{c,w} = 97615$ Hz with 1485 m/s sound velocity and assuming the plane wave propagation and wall rigidity. The cutoff mode is far in the ultrasonic range and can be neglected under the rigid wall assumption.

The magnitude responses of the liquid filled 1 m long tube measured by the laser vibrometer are presented in fig. 24

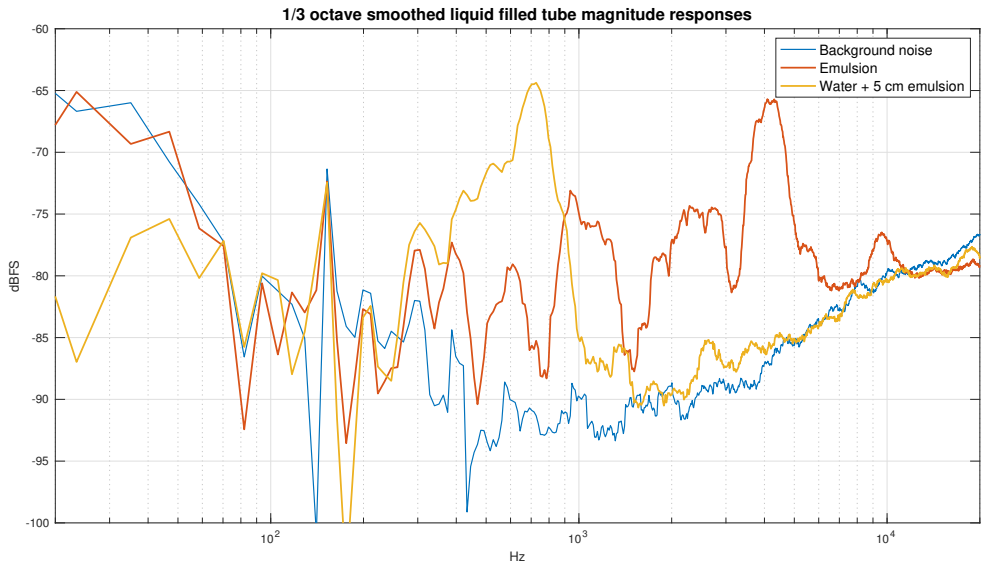

Figure 24: Magnitude responses of the 1m long tube filled with emulsion and 95 cm of water + 5 cm of emulsion.

From these measurements, it is seen that compared to the air filled tube, the sound is attenuated almost to background noise level with only 1m long tube. It is assumed that the attenuation happens due to the pressure release effect of the walls and the sound is radiated outwards. Also, viscoelastic losses in the tube material are possible.

Compared to air, water is nearly incompressible and causes the energy to flow to the tube and radiate outwards and in the tube material itself. Longer tube length would have been interesting to measure, but because of the insertion friction, longer tubes could not be filled by the available methods. No signal is seen above background noise level below 250 Hz with either liquid.

There is also no signal above 7600 Hz except for the small peak at 9600 Hz with the pure emulsion. Highest signal to noise -ratio with emulsion is achieved at 4100 Hz peak, where $\mathrm{SNR}_{\mathrm{emulsion}} = 19$ dB. For water/emulsion it is $\mathrm{SNR}_{\mathrm{water}} = 25$ dB at 725 Hz. The emulsion-filled tube shows a lot of resonant behaviour and ripple in the response. Also, it seems that the highest peak of the emulsion is shifted toward higher frequencies compared to the water/emulsion. This is assumed to happen because of different coupling to the sound source. With the water filled tube, the loudspeaker had to be placed on top of the waveguide in a simply supported manner instead of clamped connection. Also, the slight impedance mismatch between the water and emulsion is plausible to affect the response.

6.4 Attenuation inside a water filled tube

The attenuation inside a water filled tube was measured. The measurements were done by filling the tube with water and inserting the hydrophone inside of the tube. A tube with a larger inner diameter had to be used in order to fit the hydrophone inside, but the thickness-to-diameter ratio was close to the other tube ($t_1/d_1 = 0.20$ and $t_2/d_2 = 0.13$).

The hydrophone cable was coated with foam rubber in order to insulate the it from any vibrations of the tube. The sweeps were recorded in 5 cm intervals along the tube with the reference point *0 cm* being the interface point of the waveguide and tube. Measurements inside of an emulsion filled tube would have been in the interest of this study, but the emulsion was found to be too viscous for moving the hydrophone without creating air pockets. The calculated attenuation per octave band from 0 to 80 cm is presented in fig. 25.

By these measurements, largest attenuation of up to 25 dB is seen on the 500 Hz and 1000 Hz bands. For the three lowest bands 32...125 Hz no attenuation is noticed, but there is minor boost at middle distances. Highest frequencies above 1000 Hz attenuate 8 to 10 dB. At high frequencies the attenuation is inversely proportional to distance.

Magnitude responses at 0 cm and 80 cm are shown in fig. 26. By comparing figs 25 and 26 we see that the most attenuated octave bands 500 Hz and 1000 Hz correspond to the reduction of resonant behaviour in the response. This kind of reduction in resonant behaviour is something that Xu [27] reports as the tube's resonance damped by the fluid.

Compared to the laser vibrometer measurements we see that the SNR is much higher.

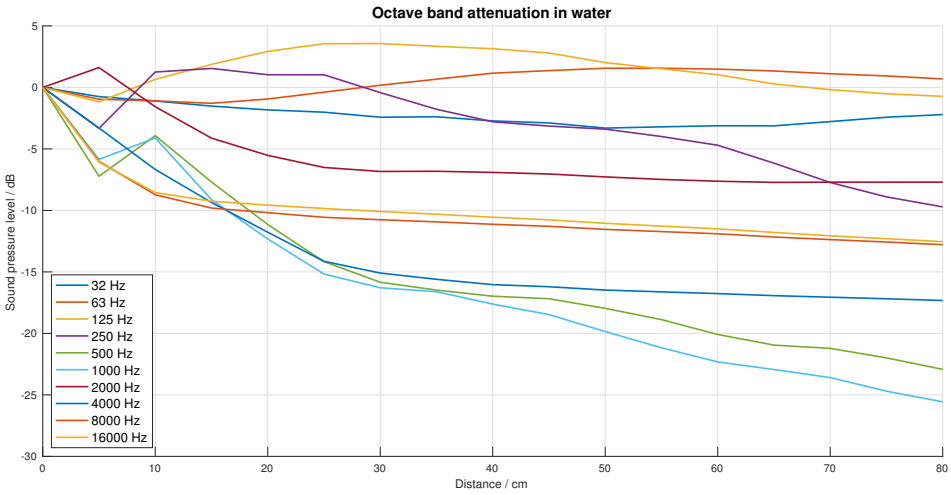

Figure 25: Attenuation inside the tube from 0 cm to 80 cm.

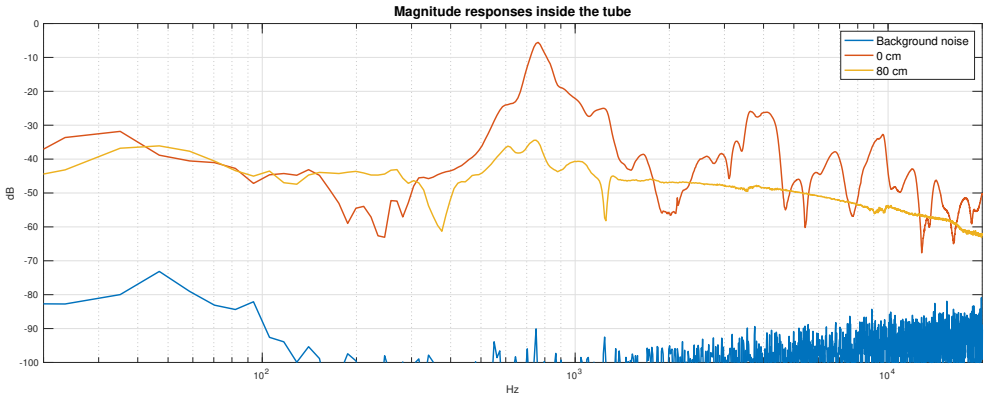

Figure 26: Attenuation inside the tube from 0 cm to 80 cm.

This is assumed to be due to the vibrometer measuring only longitudinal vibration in axial direction of the tube. The hydrophone is omnidirectional in the audible range. Differences between vibrometer and hydrophone measurements indicate that most of the longitudinally propagating sound is attenuated and the hydrophone is measuring mostly the transverse modes and coupled vibrations of the tube and liquid.

6.5 Attenuation on the surface of the tube

In addition to the other measurements, surface vibrations of the tube were measured. The hydrophone was attached firmly on the outside of the emulsion filled tube and similar to the inside attenuation measurements, the responses were recorded in 5 cm intervals, starting from the interface point of the tube and waveguide. The calculated attenuation per octave band from 0 to 80 cm is presented in fig. 27.

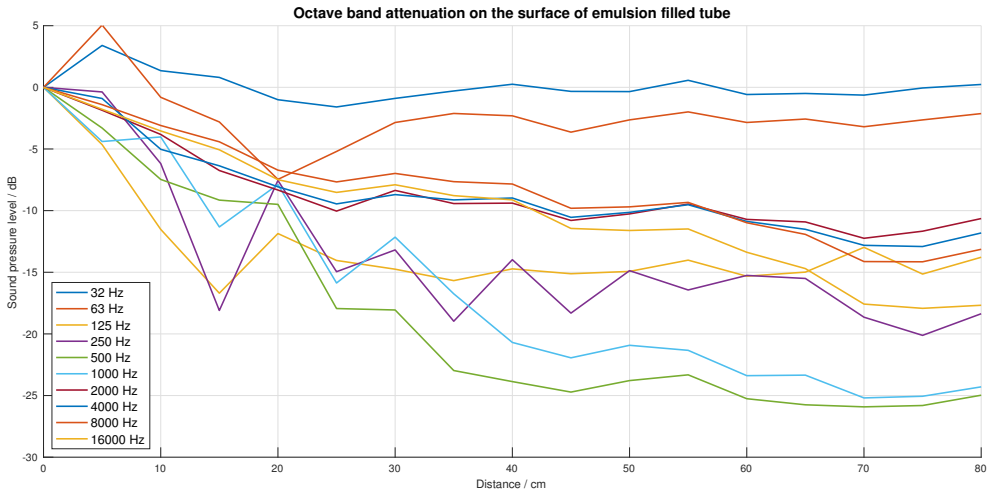

Figure 27: Attenuation on the surface of the tube from 0 cm to 80 cm.

As with the inside tube measurements, only minor attenuation is seen on the two lowest frequency bands. The largest attenuation in 500 Hz and 1000 Hz bands are the resonances being evened out in the same way as with the water-filled tube. Magnitude responses at 0 and 80 cm are presented in fig. 28. High frequencies above 2000 Hz are attenuated slightly more in comparison with the inside of water-filled tube, which is due to strong viscosity of the emulsion.

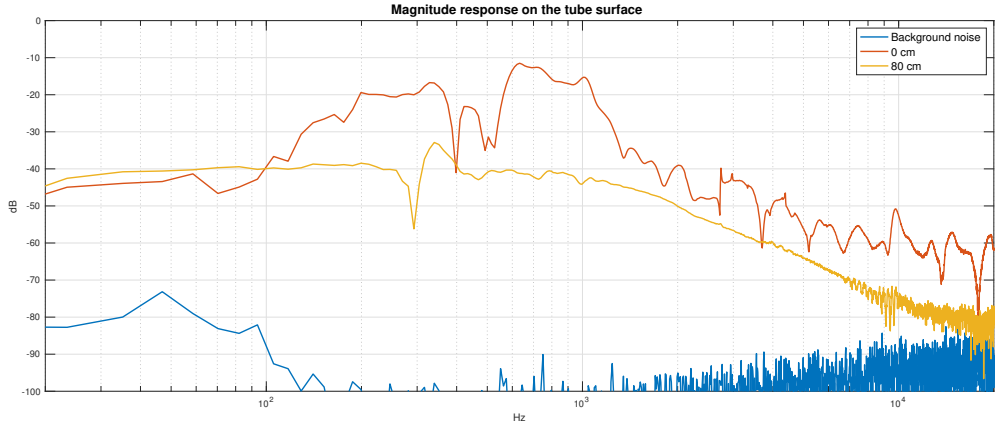

Figure 28: Attenuation on the surface of the tube from 0 cm to 80 cm.

The similar type of attenuation behavior inside and on the surface indicates a strong coupling between the liquids and tubes. The calculated mode-independent coupling parameters are $\eta_{\text{air}} = 0.004$, $\eta_{\text{water}} = 3.56$ and $\eta_{\text{emulsion}} = 3.40$ predicting strong coupling for the liquids and minimal coupling for air. The measurement results provide confirmation to the calculated coupling parameters.

7 Discussion and future work

The initial starting point for this work may be considered challenging. Sound propagation and vibration in fluid filled elastic shells is undesirable in many cases such as ventilation ducts and industrial machinery pipes. In very rare cases, sound propagation in tubes is considered desirable. There are various issues in terms of finding non-ferrous, sound insulating and acoustically high quality solutions to propagate sound to a person's ear in MRI.

It has been shown that a liquid filled flexible polymer tube has strong coupling between the liquid and shell. The coupled system has complex wave behaviour due to the pressure release effect of the tube walls. A set of more detailed measurements would be beneficial to estimate the complex modal behaviour in terms of tube-fluid interaction. They would help to evaluate whether or not the transverse waves of the system could be used to propagate good quality sound to the human ear.

The measurement results in this study suggest that the longitudinal waves in the liquid are strongly attenuated due to coupling, classical attenuation or other liquid loss types, meanwhile transverse or longitudinal waves are carried in the tube. Dispersion due to coupling and the different sound velocities at different modes of propagation have to be evaluated, as the longitudinal, transverse, extensional and flexural waves all have their designated velocities and mode dependent coupling.

The type of excitation is given importance in the literature, as the excitation to only liquid, only the shell or both affect the outcome. In this study, the excitation to the shell was insulated and evaluated in a practical manner. Piston transducers could be developed for bare liquid excitation. The maximum limit of transducer power output should also be estimated to avoid cavitation.

Properties of the liquid medium are important to reduce transmission loss. A certain degree of viscosity is needed in order to stop the liquid from leaking out of the ear. A reasonable balance between leaking and classical attenuation should be researched. Emulsions are also challenging for sound propagation. The interaction between water and oily products may absorb sound. Sound may also be attenuated by energy losses due to deformations in the structure of the emulsion. A liquid with only one chemical phase and the ability to be safely inserted in the human ear should be used. An industrial solution for filling the tube should be considered to avoid air bubbles in the liquid. Also, the effect of external static pressure to the tube would be interesting to investigate.

Properties of the elastic tube have to be considered. Measurements and detailed theoretical analysis of the outwards radiated sound power could provide insight to designing less radiating tubes. The results of this study indicate that the tube used in this work is radiating power outwards into the surrounding air. Ratio of thickness to the tube diameter could be increased to reduce radiation in middle and high frequencies within the practical limitations in MRI machines. Also more dense tube material (or less dense liquid) would improve the results. Measurements with

industrially filled tubes longer than 1 m are needed to evaluate total attenuation for required lengths. In addition, the measurements do show the pressure release effect also with the air filled tube. This encourages to minimize the length of the tube to it's minimum for the final application. Experimental tube types such as hinged carbon fiber tubes could be experimented.

Whether or not decent quality sound could be transmitted in a liquid filled tube in MRI as proposed in this thesis has to be validated by listening tests. One of the more modest requirements would be high enough speech transmission index (STI) for communication between the test subject and supervisor. The perceptual quality of sound should also be compared to the existing MRI sound systems.

8 Conclusions

This thesis has studied the possibility to transmit piezoelectrically induced sound through a liquid filled elastic tube with respect to limiting conditions in MRI scanners. The main considerations were special acoustical features of viscous liquids and the effect of pressure release walls for cylindrical shells. The phenomenon was examined through a literature study as well as several experimental measurements with laser doppler vibrometer and hydrophone at different locations along a flexible PVC tube. Air, water and viscous emulsion filled tubes were measured. The possibility to use small scale piezo transducers was also experimented.

It was found that the PVC tube and liquids exhibit strong coupling due to similar densities. Pure plane wave propagation does not exist as the longitudinal plane wave modes of the liquid are transformed to radial, circumferential, longitudinal and bending tube modes due to the pressure release effect of the tube walls. The laser vibrometer measurements of longitudinal endpoint vibration, compared to hydrophone measurements of omnidirectional vibration suggest that the longitudinal vibrations exhibit strong attenuation even for only 1 m long pressure release tubes. The pressure release effect and the low compressibility of liquids seem to guide the vibrational energy from the liquid to the shell and the shell is radiating sound outwards to the surrounding air.

Most of the attenuation occur on the frequency bands with high resonance peaks. In general the resonances and anti-resonances are smoothed out further from the sound source due to the liquid damping resonant behaviour of the tube. Only minimal viscous losses were observed at high frequencies with the emulsion compared to water. Most of the sound energy seems to propagate in the shell. Additionally, viscoelastic properties of the PVC tube are a plausible reason causing attenuation.

Small scale piezo transducers were found to produce too low output power for this application. The excitation to the tube shell should be avoided by decoupling the sound source and the shell.

The study suggests that sound cannot be transmitted through a liquid filled pressure release wall tube with good sound quality, as in the motivation of this work. More research is needed to determine if the transverse waves of the tube can be used in sound transmission with decent sound quality. Also, the impact of possible dispersion has to be taken into account. Several improvements have been proposed for the liquid properties, tube material and dimensions as well as the type of excitation to improve results with pressure release walls. Listening tests are also proposed to have a practical understanding of the sound quality at the eardrum.

References

[1] R. C. Messana, "Mri sound system transducer and headset," Jan. 11 1994. US Patent 5,277,184.

[2] S. R. More, T. C. Lim, M. Li, C. K. Holland, S. E. Boyce, and J.-H. Lee, "Acoustic noise characteristics of a 4 telsa mri scanner," *Journal of Magnetic Resonance Imaging: An Official Journal of the International Society for Magnetic Resonance in Medicine*, vol. 23, no. 3, pp. 388–397, 2006.

[3] H. F. Olson, *Acoustical engineering*. Professional audio journals, 1991.

[4] F. J. Fahy, *Foundations of engineering acoustics*. Elsevier, 2000.

[5] L. L. Beranek and T. Mellow, *Acoustics: sound fields and transducers*. Academic Press, 2012.

[6] V. Pulkki and M. Karjalainen, *Communication acoustics: an introduction to speech, audio and psychoacoustics*. John Wiley & Sons, 2015.

[7] T. D. Rossing and N. H. Fletcher, *Principles of vibration and sound*. ASA, 2004.

[8] T. D. Rossing, F. R. Moore, and P. A. Wheeler, *The science of sound. Vol. 3*. Addison Wesley, San Francisco, 2002.

[9] D. W. Robinson and R. S. Dadson, "A re-determination of the equal-loudness relations for pure tones," *British Journal of Applied Physics*, vol. 7, no. 5, p. 166, 1956.

[10] J. Blauert and N. Xiang, *Acoustics for engineers: Troy lectures*. Springer Science & Business Media, 2009.

[11] A. ANSI, "Asa s1. 1-2013 acoustical terminology," 2013.

[12] K. Oimatsu, K. Kuramoto, S. Kuwahara, and S. Yamaguchi, "Equal-loudness contours in water and its depth dependence," *Applied Acoustics*, vol. 55, no. 1, pp. 1–12, 1998.

[13] E. Meyer and E. Neumann, *Physical and Applied Acoustics, An introduction*. Academic Press, 1972.

[14] K. S. Suslick, Y. Didenko, M. M. Fang, T. Hyeon, K. J. Kolbeck, W. B. McNamara, M. M. Mdleleni, and M. Wong, "Acoustic cavitation and its chemical consequences," *Philosophical Transactions of the Royal Society of London A: Mathematical, Physical and Engineering Sciences*, vol. 357, no. 1751, pp. 335–353, 1999.

[15] J. Frenzel and H. Schultes, "Luminescence in water carrying supersonic waves," *Z. Phys. C*, vol. 27, pp. 421–424, 1934.

[16] K. F. Graff, *Wave Motion in Elastic Solids*. Courier Corporation, 1991.

[17] D. Gutierrez-Lemini, *Engineering viscoelasticity*. Springer, 2014.

[18] W. Cady, *Piezoelectricity, vols. 1 and 2*. Dover, New York, 1946.

[19] J. L. Butler and C. H. Sherman, *Transducers and arrays for underwater sound*. Springer, 2016.

[20] R. S. Woollett, *Theory of the piezoelectric flexural disk transducer with applications to underwater sound*. US Navy Underwater Sound Laboratory, 1960.

[21] L. D. Lafleur and F. D. Shields, "Low-frequency propagation modes in a liquid-filled elastic tube waveguide," *The Journal of the Acoustical Society of America*, vol. 97, no. 3, pp. 1435–1445, 1995.

[22] C. Fuller and F. J. Fahy, "Characteristics of wave propagation and energy distributions in cylindrical elastic shells filled with fluid," *Journal of sound and vibration*, vol. 81, no. 4, pp. 501–518, 1982.

[23] W. Flügge, *Stresses in shells*. Springer Science & Business Media, 2013.

[24] L. Feng, "Acoustic properties of fluid-filled elastic pipes," *Journal of Sound and Vibration*, vol. 176, no. 3, pp. 399–413, 1994.

[25] D. Paliwal, R. K. Pandey, and T. Nath, "Free vibrations of circular cylindrical shell on winkler and pasternak foundations," *International Journal of Pressure Vessels and Piping*, vol. 69, no. 1, pp. 79–89, 1996.

[26] G. Pavić, "Vibroacoustical energy flow through straight pipes," *Journal of Sound and Vibration*, vol. 154, no. 3, pp. 411–429, 1992.

[27] M. Xu and W. Zhang, "Vibrational power flow input and transmission in a circular cylindrical shell filled with fluid," *Journal of Sound and Vibration*, vol. 234, no. 3, pp. 387–403, 2000.

[28] M. Horne and R. Hansen, "Sound propagation in a pipe containing a liquid of comparable acoustic impedance," *The Journal of the Acoustical Society of America*, vol. 71, no. 6, pp. 1400–1405, 1982.

[29] W. J. Jacobi, "Propagation of sound waves along liquid cylinders," *The Journal of the Acoustical Society of America*, vol. 21, no. 2, pp. 120–127, 1949.

[30] J. James, "Computation of acoustic power, vibration response and acoustic pressures of fluid-filled pipes.," tech. rep., Admiralty Marine Technology Establishment Teddington (England), 1982.

[31] G. Morgan and J. Kiely, "Wave propagation in a viscous liquid contained in a flexible tube," *The Journal of the Acoustical Society of America*, vol. 26, no. 3, pp. 323–328, 1954.

[32] T. Lin and G. Morgan, "Wave propagation through fluid contained in a cylindrical, elastic shell," *The Journal of the Acoustical Society of America*, vol. 28, no. 6, pp. 1165–1176, 1956.

[33] R. Kumar and R. Stephens, "Dispersion of flexural waves in circular cylindrical shells," *Proc. R. Soc. Lond. A*, vol. 329, no. 1578, pp. 283–297, 1972.

[34] J. Zemanek Jr, "An experimental and theoretical investigation of elastic wave propagation in a cylinder," *The Journal of the Acoustical society of America*, vol. 51, no. 1B, pp. 265–283, 1972.

[35] J. Cuschieri, "Excitation and response of piping systems," *The Journal of the Acoustical Society of America*, vol. 83, no. 2, pp. 641–646, 1988.

[36] A. Causse and J. Trolle, "Dynamic analysis of nuclear plant circuit by vibrational intensity measurement," in *INTER-NOISE and NOISE-CON Congress and Conference Proceedings*, no. 4, pp. 579–582, Institute of Noise Control Engineering, 1988.

[37] K. Sato and I. Honda, "Application of vibrational power measurement to the piping system in an air-conditioner," in *INTER-NOISE and NOISE-CON Congress and Conference Proceedings*, no. 4, pp. 591–594, Institute of Noise Control Engineering, 1988.

[38] V. Del Grosso, "Analysis of multimode acoustic propagation in liquid cylinders with realistic boundary conditions–application to sound speed and absorption measurements," *Acta Acustica united with Acustica*, vol. 24, no. 6, pp. 299–311, 1971.

[39] A. Standard, "s1. 11-2004: Specification for octave band and fractional octave band analog and digital filters," *American National Standards Institute*, 2004.

[40] R. A. Fine and F. J. Millero, "Compressibility of water as a function of temperature and pressure," *The Journal of Chemical Physics*, vol. 59, no. 10, pp. 5529–5536, 1973.

[41] S. Kalaga and M. K. Neelam, "Elastic properties of pvc pipes," *Journal of Structural Engineering (Madras)*, vol. 29, 07 2002.

A Measurement setup photos

(a) (b)

Figure A1: Underwater loudspeaker, waveguide and the tube from top to down (a) and laser vibrometer head pointing to the end of the liquid filled tube. (b)